arXiv:2206.12838v1 [astro-ph.SR] 26 Jun 2022

Ultraviolet Spectropolarimetric Diagnostics of Hot Star Magnetospheres

A. ud-Doula[1], M. C. M. Cheung[2], A. David-Uraz[3,4], C. Erba[5], C. P. Folsom[6], K. Gayley[7], Y. Nazé [8], C. Neiner[9], V. Petit[10], R. Prinja[11], M. E. Shultz[10], N. Sudnik[12], J. S. Vink[13] and G. A. Wade[14]

*Corresponding author(s). E-mail(s): asif@psu.edu;

Abstract

Several space missions and instruments for UV spectropolarimetry are in preparation, such as the proposed NASA MIDEX Polstar project, the proposed ESA M mission Arago, and the Pollux instrument on the future LUVOIR-like NASA flagship mission. In the frame of Polstar, we have studied the capabilities these observatories would offer to gain information on the magnetic and plasma properties of the magnetospheres of hot stars, helping us test the fundamental hypothesis that magnetospheres should act to rapidly drain angular momentum, thereby spinning the star down, whilst simultaneously reducing the net mass-loss rate. Both effects are expected to lead to dramatic differences in the evolution of magnetic vs. non-magnetic stars.

1 Introduction

1.1 Background

The hot, massive stars of the upper main sequence are dominant objects in a galaxy. While much less numerous than cooler stars, they exert a wide-ranging influence on galactic structure and stellar ecology. The majority of the periodic table – all elements up to iron (Johnson, 2019) – is forged in their cores, with heavier elements being synthesized in their deaths in Type II supernovae, at which point the enriched material is returned to the interstellar medium (ISM). With tens to hundreds of thousands of times the luminosity of the Sun, and much higher temperatures with spectra peaking in the far ultraviolet (FUV), they contribute most of the ISM's ionizing radiation.

Their high luminosities launch powerful, radiatively driven winds with mass loss rates thousands to billions of times the Sun's to terminal velocities of thousands of km/s, injecting substantial matter and momentum into the ISM.

The combination of ionizing radiation and powerful stellar winds hollows out star-forming material, quenching star formation. Upon supernova detonation at the end of a hot star's life, the resulting shock wave contributes a final burst of rapidly moving material that can trigger star formation by initiating the gravitational collapse of nearby molecular clouds. Following the supernova, the stellar remnant begins an extended afterlife as a neutron star or black hole, long-lived objects that – in the deep cosmic future – will be one of the few inhabitants of the cosmos (Renedo et al, 2010;

Slane et al, 2016; Cosentino et al, 2022; Grudić et al, 2022; Adams and Laughlin, 1997).

The structure and evolution of single stars are largely functions of the stellar mass, therefore any process that changes the mass will change the evolution of the star. For O-type stars, which have mass-loss rates of around 10^{-6} M$_\odot$ yr^{-1}, main-sequence lifetimes on the order of 10 Myr, and initial masses of around 50 M$_\odot$, mass loss via stellar winds can result in considerable reductions in mass. The evolution of such stars therefore cannot be understood in isolation from the effects of their wind, since differences in the terminal, pre-supernova state of a star have consequences for the type of supernova as well as the type of remnant that emerges.

Many massive stars are rapid rotators, with equatorial surface rotational velocities of hundreds of km/s. In the most extreme cases, stars may rotate near their critical or breakup velocities, leading to deformation of their shape from a spherical to an oblate form, bulged around the equator, with much cooler equatorial temperatures due to gravity darkening (von Zeipel, 1924). Even in less extreme cases, rotation leads to mixing, replenishing the nuclear-burning core with fresh material from the envelope, and thereby having a strong effect on the evolution of the star (e.g. Brott et al, 2011).

Due to the dominant role played by massive stars in terms of mass and energy input via winds, ionizing radiation, and supernovae, understanding the evolution of galaxies requires understanding the evolution of massive stars, which in turn requires that we understand their winds and their rotation along with all phenomena that can modify these key parameters.

It is clear that there is no such thing in nature as a really 'normal' or 'standard' massive or hot star. Instead, there is a diversity of special cases, such as classical Be stars, interacting binaries, or magnetic hot stars, which collectively comprise the hot star population. It is only via understanding of the properties of these individual groups that the properties of the massive stars can be properly accounted for in population synthesis models, which in turn are key inputs for models of galactic chemical and structural evolution.

Main focus of this paper is understanding the properties of the special group of magnetic hot stars. The proposed Polstar NASA MIDEX mission will greatly help us achieve this goal, as it is equipped with a 60-cm telescope and a full-Stokes (IQUV) spectropolarimeter divided in 2 channels in the ultraviolet with the first one providing spectropolarimetry at high spectral resolution of R∼33000 over the 122-200 nm far-UV bandpass and the second one providing spectropolarimetry over the 180-320 nm NUV band with low- to mid-resolution (R∼30 to 250) (Scowen et al, 2021). Thus, Polstar is quite well suited for studying hot stars and their circumstellar environment.

In the remainder of this section, general background is provided on hot star magnetic fields, magnetospheres, magnetospheric diagnostics, and the effects of magnetospheres on stellar evolution, culminating with the motivation for exploring these effects with Polstar. The known properties of ultraviolet magnetospheric diagnostics, a comparison with visible and X-ray diagnostics, and an overview of the simulations and models used to interpret them, are given in Sect. 2. Expectations for linear spectropolarimetry arising from scattering in the circumstellar environment, drawing on both models and observations acquired with high-resolution visible instrumentation, are described in Sect. 3. Linearly polarized broadband magnetospheric signatures, again drawing on both models and observations, are given in Sect. 4. Enabled science falling under the purview of magnetic and magnetospheric activity in hot stars is described in Sect. 5. The paper is summarized in Sect. 6.

1.2 Massive star magnetism

Magnetic fields are a crucial factor that leads to drastic modifications in both the mass-loss rates and rotation of hot stars. They are found in approximately 10% of the OBA population (Grunhut et al, 2017; Schöller et al, 2017; Sikora et al, 2019). The magnetic fields of stars with radiative envelopes share similar properties from approximately spectral type A5 to the top of the main sequence (Donati and Landstreet, 2009). They are strong (ranging from hundreds of G to tens of kG; Shultz et al, 2019), they are stable over timescales of at least decades (Shultz et al, 2018), and they are globally organized and, with few exceptions, geometrically simple (being well-described by tilted dipoles with most of the magnetic energy in low-order poloidal field

components; Kochukhov et al, 2019). Magnetohydrodynamic simulations have demonstrated that such fields, once established, can remain stable over evolutionary timescales (e.g. Braithwaite and Spruit, 2004), leading to the hypothesis that they are of 'fossil' origin i.e. remnants of some previous event in the star's life (Donati and Landstreet, 2009).

Moreover, since there is no correlation of magnetic field strengths with rotational or stellar properties, as expected and observed for the dynamo fields of cool stars (e.g. Folsom et al, 2016; Shulyak et al, 2017), and as there is furthermore no known dynamo mechanism capable of sustaining globally organized magnetic fields in the radiative atmospheres of hot stars, it supports further our belief that these magnetic fields are indeed fossils arising in some earlier phase of the star's life (Donati and Landstreet, 2009), e.g. due to amplification of ISM seed fields during formation and/or convective phases during pre-main sequence evolution (e.g. Villebrun et al, 2019), or in dynamos powered by binary mergers (e.g. Schneider et al, 2019). An improved understanding of the formation mechanism of fossil fields therefore offers the promise of advancing our general understanding of the formation or evolution of hot stars.

While strong fields are relatively rare in more massive OBA stars, weak fields may be widespread. The detection of 'ultra-weak' ($\sim$0.1-10 G) magnetic fields in a number of bright A-type stars suggests that magnetic phenomena may be ubiquitous on the upper main sequence (Blazère et al, 2020). Weak magnetic fields have also been detected in numerous blue supergiants, indicating that they may play a role in post-main sequence evolution as well (Neiner et al, 2017; Martin et al, 2018; Oksala et al, 2021). These weak fields are expected to arise from small-scale dynamos powered by embedded helium and iron opacity-bump convection zones (Jermyn and Cantiello, 2020), which are revealed as the stellar wind strips away the outer layers of the star (Jermyn and Cantiello, 2021). However, in more massive OB stars, even if weak magnetic field incidence were to be found ubiquitous, their influence is expected to be dynamically negligible due to a much stronger wind or equivalently to much higher mass loss rates.

1.3 Massive star magnetospheres

Strong magnetic fields are easily capable of trapping the ionized wind of a massive star (ud-Doula and Owocki, 2002). The surface mass flux from opposite magnetic colatitudes is channeled by the magnetic field and collides in the magnetic equatorial plane, leading to the accumulation of a torus of high-density plasma surrounding the magnetic equator, with X-rays produced in the cooling shocks (ud-Doula et al, 2014a).

Magnetic confinement extends out to the Alfvén surface, the distance from the star at which the magnetic energy density and the kinetic energy density of the wind equalize, with the Alfvén radius R_A defined in the magnetic equatorial plane. Alfvén radii commonly range from a few stellar radii (as is typical for an O-type star, where the powerful wind rapidly overpowers the magnetic field) to tens of stellar radii (as is typical for a strong magnetic field trapping the much weaker wind of a B-type star).

Beyond the Alfvén surface, the wind is magnetically unconfined and escapes from the star. Below the Alfvén surface, plasma is forced into corotation with the stellar magnetic field by the Lorentz force. If a star is slowly rotating, gravity pulls the confined dense plasma back to the star. This can dramatically reduce the net mass-loss rate of the star (ud-Doula and Owocki, 2002; Petit et al, 2017). If a star is rapidly rotating, such that the Kepler corotation radius R_K (at which gravity is balanced by the centrifugal force imparted by corotation) is inside the Alfvén radius, gravitational infall is prevented in the part of the magnetosphere above R_K. The former case is referred to as a *Dynamical Magntosphere* (DM) since mass-balancing occurs on dynamical timescales; the latter case is referred to as a *Centrifugal Magnetosphere* (CM; Petit et al, 2013). Importantly, all magnetic stars have DMs in at least the inner part of the magnetosphere[1].

Plasma inside a CM is unable to fall back to the star, and 2D magnetohydrodynamic (MHD) simulations indicate that it will instead build up until it reaches a critical density beyond which

---

[1]Unless the star is critically rotating, in which case R_K becomes identical to the equatorial radius; while theoretically possible, no such object has been found, and in any case such a phase would be extremely short-lived due to strong magnetic braking.

the magnetic field is unable to confine it, at which point it is ejected outwards – a phenomenon referred to as centrifugal breakout (ud-Doula et al, 2008). However, more recent 3D MHD simulations indicate such breakout events occur continuously and on a smaller scale (ud-Doula, 2020). This mass-balancing mechanism has been verified via analysis of the Hα emission properties of stars with CMs (Shultz et al, 2020; Owocki et al, 2020). Thus, plasma accumulated in the DM is trapped and returned to the star, whereas plasma trapped in the CM will eventually be lost; only the CM reduces the net mass-loss rate.

Poynting stresses in the magnetosphere lead to rapid angular momentum loss (ud-Doula et al, 2009), as a result of which magnetic hot stars are systematically more slowly rotating than non-magnetic stars of comparable spectral type and luminosity class (Shultz et al, 2018). In some cases, the rotational period change can be directly measured (Townsend et al, 2010). Rotational spin-down can be so extreme that rotational periods of up to decades in length have been identified (e.g. Nazé et al, 2010; Shultz and Wade, 2017; Shultz et al, 2017; Erba et al, 2021b). An important consequence of this is that the CM quickly shrinks as a star ages, and is detectable only during the initial phase of the main sequence (Shultz et al, 2019).

1.4 Multiwavelength magnetospheric diagnostics

In addition to their important consequences for stellar evolution, magnetospheres have a number of observational consequences. There are available diagnostics across the electromagnetic spectrum, each of which probes a different magnetospheric component, and is detectable in a different part of stellar and magnetospheric parameter space.

X-rays are emitted due to magnetically confined wind shocks, making magnetic stars much more luminous in X-rays than non-magnetic stars (e.g. Nazé et al, 2014; ud-Doula et al, 2014a). While X-rays are detectable for most magnetic OB stars, time series data are difficult to acquire.

Velocity-resolved information from line emission is furthermore difficult to obtain for all but the brightest X-ray sources. However, in 2031 the launch of the *Athena* mission will in fact provide velocity-resolved X-ray information (Nandra et al,

2013), which may provide a powerful complement to the data gathered by Polstar (although the science case presented here is independent of any results from Athena).

Rapidly rotating magnetic AB stars[2] can exhibit radio gyrosynchrotron emission originating at high magnetic latitudes (e.g. Leto et al, 2021), beamed auroral radio emission via the electron cyclotron mechanism (e.g. Das et al, 2021), and line emission in near infrared and visible Bracket, Paschen, and Balmer series H lines, most prominently in Hα (e.g. Grunhut et al, 2012; Oksala et al, 2015a).

Since the weak winds of B-type stars are unable to fill their DMs to sufficient density to become optically thick in Hα (Petit et al, 2013), their magnetospheres are detectable in visible data only around young, rapidly rotating, strongly magnetic stars with large CMs, which due to rapid magnetic braking disappear after less than 1/3 of the stars' main sequence lifetime (Shultz et al, 2019).

By contrast, ultraviolet signatures associated with magnetospheres have been detected across the Hertzsprung-Russell diagram, making FUV resonance lines the most versatile and ubiquitous diagnostic by far. These lines probe both the free, unconfined stellar wind, and the dynamical magnetosphere (e.g. Shore and Brown, 1990; Marcolino et al, 2013; Petit et al, 2013; Erba et al, 2021a). However, the C IV wind lines persist to B3 or so, and below that wind signatures disappear in resonance lines (Slettebak, 1994). While Oksala et al (2015b) showed that modelling of the equivalent width of SiIV line could plausibly be reproduced with a photospheric model, they did not give detailed line profile models. But, in general, UV diagnostics provide information on that part of the wind which is escaping, and that part which is returned, to the star. UV resonance line variability is almost universally detectable in magnetic OB stars (e.g. Henrichs, 2001; Schnerr et al, 2008; Henrichs et al, 2012, 2013; David-Uraz et al, 2019a; Erba et al, 2021b). It therefore provides the only diagnostic that a) can be used for magnetic stars across the full range of magnetic, rotational,

---

[2]This diagnostic is unavailable for O-type stars, since the large radio photospheres produced by their dense winds swallow any gyrosynchrotron radiation produced by their magnetospheres (e.g. Chandra et al, 2015).
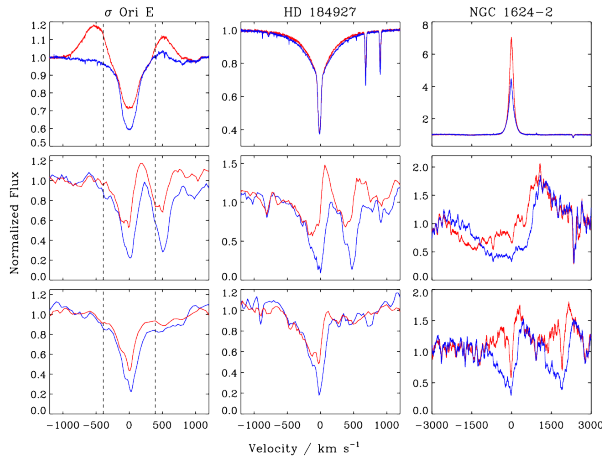
Fig. 1 Comparison of Hα (top), the C IV λλ1548,1551 doublet (middle), and the Si IV λλ1394,1403 doublet (bottom) for 3 representative stars (note that the red component of the Si IV is not visible for σ Ori E and HD 184927). High and low state are respectively indicated by red and blue. For σ Ori E, dashed lines indicate $\pm R_{\mathrm{K}}$. All lines have been shifted to the stellar rest frame. For more details, see for instance Wade et al (2012)

and stellar parameters, b) provides simultaneous information on the wind and the magnetosphere, and c) provides velocity-resolved information with which the detailed magnetospheric structure can be examined.

The application of UV spectroscopy to the study of hot star magnetospheres is conceptually similar to its utility in the study of the solar magnetosphere. One recent example is the IRIS mission, which has been obtaining high resolution FUV spectroscopy of solar plasmas since 2013. The FUV band of IRIS regularly observes the same Si IV doublet that is used to probe the winds of hot stars. In the solar case where Si IV line profiles are in pure emission, these profiles are used to probe Doppler flows of plasmas at $T \sim 80$ kK (e.g. Cheung et al, 2015).

2 UV spectroscopic diagnostics of massive star magnetospheres

The interest of UV observations has been well demonstrated in the study of magnetic O stars (e.g. Smith and Fullerton, 2005; Grunhut et al, 2009; Marcolino et al, 2012, 2013; Nazé et al, 2015; David-Uraz et al, 2019a, 2021). As UV line profiles trace the density and velocity structure of the wind along the line-of-sight, line profile variations are expected for magnetic stars as the stellar rotation modifies the observer's viewing angle of the non-spherical magnetosphere. The available observations reveal enhanced absorption at low-velocity where the slow, confined wind appears in front of the star (equator-on view). In contrast, high-velocity absorption is recorded for optically-thick lines where the fast, polar wind enters the line-of-sight (pole-on view). These differences between pole-on and equator-on observations are magnified for extremely magnetic stars (such as NGC 1624-2), or are totally damped in the case of very weakly magnetic stars (e.g., ζ Ori A). However, they are qualitatively reproduced by dedicated models that in general assume simple dipolar magnetic field topology (Marcolino et al, 2013; Nazé et al, 2015; Erba et al, 2021a) indicating a smooth transition between these two phases.

But additional observational datasets obtained at different stellar rotational phases reveal clear departures from such a smooth transition (David-Uraz et al, 2021). Furthermore, for some cases, the UV lines profiles along opposite poles exhibit significant differences (Nazé et al, 2015), indicating a more complex magnetospheric geometry than the generally assumed simple dipoles. By observing a large sample of stars with a dense phase coverage, Polstar will reveal the magnetic topology more accurately.

UV spectroscopy has also been crucial to detecting and understanding the magnetospheres of B-type stars (e.g. Smith and Groote, 2001; Neiner et al, 2003a,b; Donati et al, 2006a; Schnerr et al, 2008; Petit et al, 2011; Henrichs et al, 2013; Erba et al, 2021b), including the ones lacking the surface chemical peculiarities characterizing the universally magnetic Bp class (e.g. Neiner et al, 2003a; Donati et al, 2006a; Petit et al, 2011; Shultz et al, 2017). As surface chemical abundance patches are unable to form when the stellar wind strips the surface faster than patches can accumulate, these anomalous ultraviolet lines enabled successful identification of magnetic stars earlier than B2, as in the case of β Cep (Henrichs et al, 2013), τ Sco (Donati et al, 2006b), or the τ Sco analogues (Petit et al, 2011).

As with magnetic O-type stars, magnetic B-type stars exhibit periodic variations modulated on the rotational timescale. Observationally, the UV lines of magnetic B stars are characterized

by a 'high state' with a red-shifted emission feature and a blue-shifted absorption, similar to a the classical P-Cygni profile originating in a spherically expanding wind, but appearing at much cooler effective temperatures than those at which P-Cygni profiles are generally seen. At 'low state', the red-shifted emission disappears and the blue-shifted emission becomes stronger. The high state corresponds to the maxima of $\langle B_z \rangle$, the line-of-sight magnetic field averaged over the visible stellar hemisphere, i.e. high state is seen when the magnetic pole is closest to the line of sight. On the other hand, low state corresponds to $\langle B_z \rangle$ nulls, i.e. when the magnetic equator is along the line of sight. In terms of modeling, this is generally interpreted as a result of a plasma torus in the magnetic equatorial plane, which either produces emission when viewed pole-on, or absorption when the torus eclipses the star in equator-on view.

Magnetic B-type stars frequently display variability in the N v 123.9, 124.3 nm doublet. These lines are not easily produced in such stars since the ionization temperature of N iv is higher than their photospheric effective temperature. This is believed to be due to over-ionization from X-rays produced in colliding wind shocks (e.g., Smith and Groote, 2001; ud-Doula et al, 2014a), and is entirely absent in non-magnetic B-type stars. As such, this doublet can provide us with a clear diagnostics for magnetism in B-type stars. NLTE calculations, like those done in another context by Carneiro et al (2016), will be required before a full understanding is achieved.

2.1 Visible versus Ultraviolet Magnetospheric Diagnostics

Fig. 1 compares the variable magnetospheric line diagnostics available from Hα to two UV resonance lines, the C iv 154.8, 155.1 nm and Si iv 139.4, 140.3 nm doublets.

In the case of the CM star σ Ori E (B2 Vp; Abt and Levato, 1977), Hα emission variability is predominantly located outside of the Kepler corotation radius (indicated with vertical dashed lines), a consequence of the accumulation of cool, dense plasma at and beyond $R_{\rm K}$ which, at high state, is projected off of the stellar limb. By contrast, neither of the UV doublets demonstrate any variable emission outside of $\pm R_{\rm K}$. Instead, there is an emission feature shifted to the red of the line

center. At low state, the high-velocity emission disappears in Hα, replaced by enhanced absorption in the line core; this is due to the CM eclipsing the star (e.g., Sundqvist et al, 2012; ud-Doula et al, 2013). Similar enhanced absorption, also due to eclipsing, is detectable in the UV during low state. Note that the amplitude of variation is largest in the C iv doublet, however as the two components are very close to one another their emission overlaps, whereas the Si iv doublet has weaker emission, but the larger separation of its components enables the contribution of each line to be more effectively isolated.

There is no Hα emission in the case of HD 184927 (B2 Vp; Yakunin et al, 2015): while this star has a similarly strong magnetic field to that of σ Ori E, it has a much longer rotational period and, therefore, does not possess a large CM. Its UV variability is however remarkably similar to that of σ Ori E. Together with the absence of UV variations outside the Kepler radius in σ Ori E's UV lines, this suggests that, amongst B-type stars, the UV is primarily probing the dynamical part of the magnetosphere, i.e. the region closest to the star (e.g. Petit et al, 2013).

The O-type star NGC 1624-2 has the strongest magnetic field of any star at the top of the main sequence ($B_{\rm p} \sim 20$ kG; Wade et al, 2012). Its long rotational period (~ 158 d) means that its magnetosphere is purely dynamical (Petit et al, 2013). Its Hα line shows extremely strong emission at high state, due to its large Alfvén radius and the powerful wind that easily fills the DM. Hα emission is only slightly weaker during low state. The emission is confined within about ± 200 km s^{-1} of line centre. The velocity broadening is expected to be primarily thermal and turbulent, and the low velocity of the material again reflects the fact that Hα is probing the dense, cool plasma around the magnetic equator (e.g., Sundqvist et al, 2012). By contrast, NGC 1624-2's UV profiles demonstrate both strong emission and absorption (David-Uraz et al, 2019a, 2021). The C iv doublet provides a sensitive probe of the unconfined wind, as revealed by its P Cygni-like profile, whereas Si iv is apparently more sensitive to the magnetically confined plasma.

Fig. 1 demonstrates two important advantages of the UV: 1) unlike Hα, UV emission is

detectable for essentially all magnetic stars earlier than B2; 2) even when Hα is available, UV emission probes magnetospheric regions that are not reachable by other means. The relevance of UV diagnostics to the characterization of hot star magnetospheres underscores the importance of innovative UV observatories, such as the proposed Polstar mission.

2.2 X-ray versus Ultraviolet Magnetospheric Diagnostics

Relatively strong magnetic fields channel wind towards the magnetic equator where they collide. The resultant strong shock is able to generate hard X-ray emission, in addition to the soft X-rays naturally generated in all magnetic stars earlier than about B3 winds due to the Line-Deshadowing Instability (LDI) (Babel and Montmerle, 1997; Owocki et al, 1988; Driessen et al, 2021). For example, in non-magnetic O-stars, LDIs generate soft X-ray emission with a luminosity scaling with the bolometric one ($L_X/L_{BOL} \sim 10^{-7}$, Berghoefer et al 1996; Feldmeier et al 1997) while the magnetic O-stars show a clear enhancement, (with $\log[L_X/L_{BOL}] \sim -6.2$; Nazé et al 2014; Oskinova et al 2011). For most B-stars, the X-ray luminosity and its ratio with respect to bolometric luminosity are smaller. However, as for O-stars, they agree well with the predictions of the X-ray Analytic Dynamical Magnetosphere (XADM) model (Nazé et al 2014; Owocki et al 2016; Fletcher et al 2018). However, a few discrepancies remain and require data at other wavelengths – especially in the UV – to understand the peculiarities of the magnetospheres of these targets (e.g. the complex magnetic geometry of τ Sco, or the potential impact of fast rotation) and the exact temperature stratification (to understand notably why X-rays are not as hard as predicted see e.g. HD 191612, Nazé et al 2016, or to understand notably the diversity in X-ray hardness and variability behaviours (Nazé et al 2014).

In a few cases (e.g., θ^1 Ori C, Gagné et al 2005; HD 191612, Nazé et al 2010 ; CPD –28 2561, Nazé et al 2015; NGC 1624-2, Petit et al 2015), sufficient X-ray data were collected to detect variability of the X-ray flux with the rotational period. Only the extremely magnetic NGC 1624-2 showed a clear increase of absorption when the confined winds were seen magnetic equator-on, demonstrating

that the X-ray emitting source lies in the confined winds, and that their cool component can be dense enough to absorb X-rays. Other objects, in general, are subject to occultation effects wherein the X-ray emission directly behind the star is hidden as the confined winds are viewed magnetic equator-on. In some cases, large amount of X-ray variability suggests that the X-ray emitting region is not symmetric, as in a ring (ud-Doula and Nazé, 2016). However, additional information potentially due to UV polarimetry from Polstar will enable determination of the exact magnetospheric geometry and help us model them more precisely, leading to better constraints in X-rays as well.

Very few magnetic stars can be studied at high-resolution in X-rays because of the low sensitivity of such facilities (although this may change when Athena becomes operative). The narrow and symmetric X-ray lines agree with predictions of magnetohydrodynamic (MHD) models (Mewe et al, 2003; Gagné et al, 2005; Nazé et al, 2007, 2008, 2012; Favata et al, 2009), but a detailed, quantitative assessment of the plasma kinematics can only be done at other wavelengths. A careful and systematic study of these magnetospheres in UV with missions such as proposed Polstar represents a unique opportunity to better understand these objects.

2.3 Numerical Modeling of Hot Star Magnetospheres

Some characteristics of UV observations can be predicted by numerical models of hot star magnetospheres. In the past two decades, extensive observational surveys supported by theoretical analyses provided a strong basis to develop a successful general paradigm for characterizing the properties of hot star magnetospheres in terms of their rotation (setting the Kepler co-rotation radius R_K) and level of wind magnetic confinement (setting the Alfvén radius R_A; see figures 2 and 3).

As with X-rays, MHD simulations have been used advantageously to reproduce the overall variability phenomenology of UV resonance lines (Marcolino et al, 2013; Nazé et al, 2015). As a sample of a fully self-consistent 3D MHD simulation of a hot star magnetosphere, figure 4 (ud-Doula et al, 2013) shows how wind material
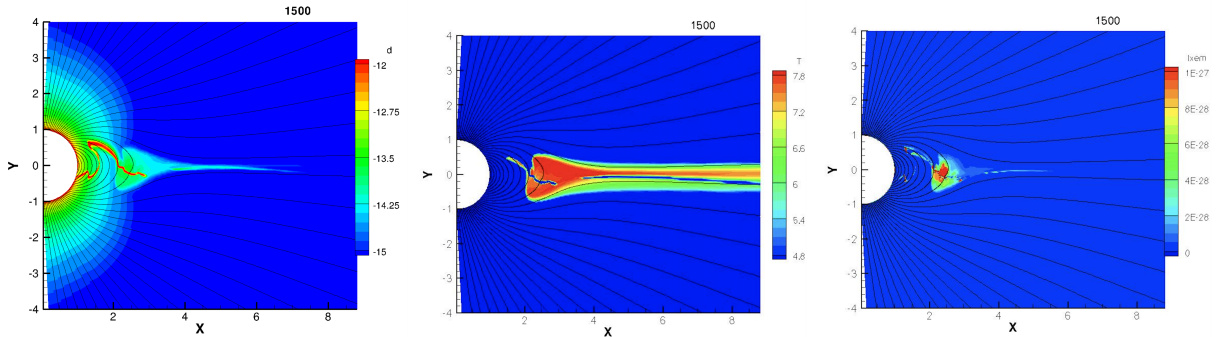
Fig. 2 For a 2D MHD simulation of a magnetized wind with confinement parameter $\eta_* = 100$, color plots of log density (left) and log temperature (middle) in cgs units for arbitrary snapshot many dynamical times after initialization. Note that magnetic loops extending above $R_A/R_* \approx 100^{1/4} \approx 3.2$ are drawn open by the wind, while those with an apex below R_A remain closed. The right panel plots associated X-ray emission from the magnetically confined wind shock (MCWS) near the apex of closed loops. Figure adopted from ud-Doula et al (2014b).

trapped in closed loops over the magnetic equator in θ^1 Ori C (left panel) leads to circumstellar emission that is strongest during rotational phases corresponding to pole-on views (middle panel). For a pure dipole with the inferred magnetic tilt $\beta = 45°$, an observer with the inferred inclination $i = 45°$ has perspectives that vary from magnetic pole to equator, leading in the 3D model to the rotational phase variations in the Hα equivalent widths shown in the right panel (shaded circles). Such models can also help us synthesize UV line profiles that Polstar can observe.

Additionally, dynamic flows formed in the DM as material is launched from the surface and then falls back in complex patterns, occurring on timescales of tens of ks (ud-Doula et al, 2008), could lead to small-scale stochastic variability in several diagnostics. This was tentatively detected for θ^1 Ori C (ud-Doula et al, 2013), in which short-timescale variability is found in the equivalent width measurements of Hα, on top of larger, rotationally-modulated variations. However, such short-term variability has yet to be detected in the UV, as no magnetic star has been observed with sufficiently closely-spaced or high-SNR spectroscopic time-series. To best disentangle the various scales of variability that might arise as a consequence of dynamic flows in the DMs of magnetic massive stars, targets with very dense DMs and very slow rotation (such as HD 108; Martins et al, 2010; Shultz and Wade, 2017) appear most promising.

2.4 Analytical Models of Highly Magnetized Hot Star Winds

Ultimately, proper self-consistent treatment of the global mass budget, including complex cycles of upflow and infall in DMs, and eventual *centrifugal breakout* (CBO) of trapped plasma in CMs, requires self-consistent MHD simulations that account for the competition between field and material flow. However, in the limit of arbitrarily strong fields (effectively with $R_A \to \infty$), analyses based on an idealization of purely rigid fields have led to both the *Analytic Dynamical Magnetosphere* (ADM) and *Rigidly Rotating Magnetosphere* (RRM) models that have shown great promise for analyzing broad observational trends in multiple diagnostics, without the computational complexity and expense of full MHD simulations.

Townsend et al (2005) have shown that the RRM model can successfully reproduce the periodic modulations observed in the light curve, Hα emission-line profile, and longitudinal field strength of σ Ori E, a rapidly rotating, strongly magnetized star with a large CM. In this model, plasma accumulates at minima within the gravitocentrifugal potential of a rotating star, which define a warped accumulation surface approximately in the magnetic equatorial plane, with the densest regions at the intersections of this plane with the rotational equatorial plane, and an inner edge approximately defined by the Kepler corotation radius R_K (with a gap between R_K and the star). The model can be extended from a
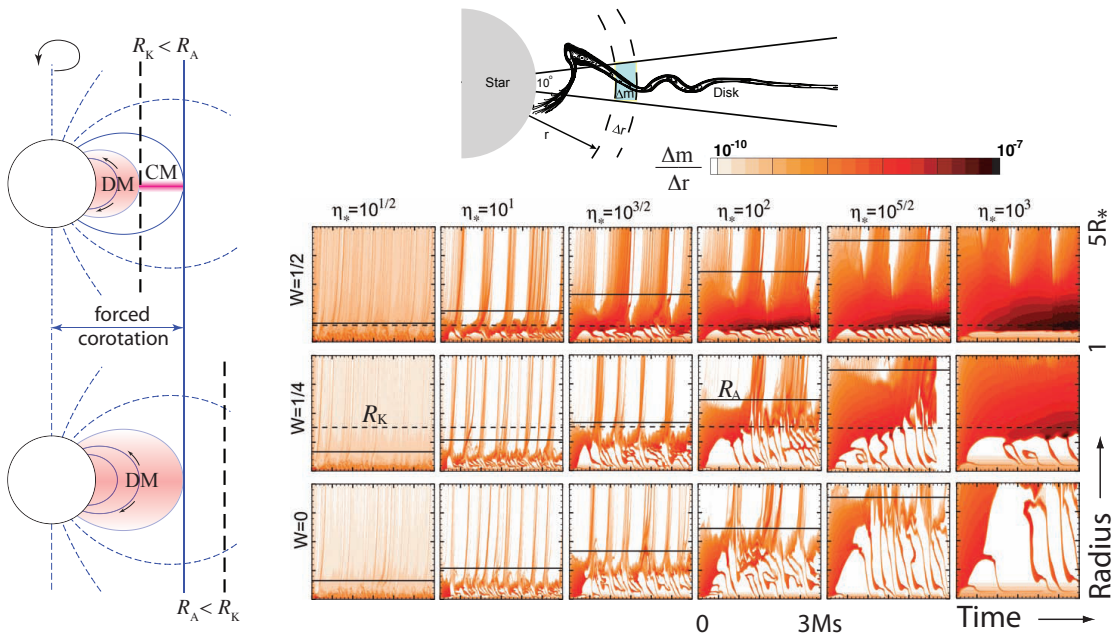
Fig. 3 *Left:* Sketch of the regimes for a dynamical vs. centrifugal magnetosphere (DM vs. CM). *Upper right:* Contour plot for density at an arbitrary snapshot of an isothermal 2D MHD simulation, overlaid with illustration to define the logarithm of radial mass distribution, $\Delta m/\Delta r$ near the equator in the unit of solar mass per stellar radius. *Lower right:* Color plots for log of $\Delta m/\Delta r$, plotted versus radius (1-5 R_*) and time (0-3 Msec), for a mosaic of 2-D MHD models with a wide range of magnetic confinement parameters η_*, and 3 orbital rotation fractions W. The horizontal solid lines indicate the Alfvén radius R_{Alfven} (solid) and Kepler radius R_{Kepler} (dashed). Figure adopted from ud-Doula et al (2008).

simple tilted dipole to any arbitrary magnetic geometry, e.g. as determined via ZDI, a method which Oksala et al (2015b) used to reproduce the spectroscopic and photometric properties of the prototypical magnetic star σ Ori E. The RRM model has also been used to predict the broadband polarimetric observables of σ Ori E, although in this case there is severe tension between the best fit achieved by polarimetry and photometry (Carciofi et al, 2013, see also Sect. 4).

The ADM model (Owocki et al, 2016) was developed to provide an approximate, static view of the magnetospheric structure of a slowly-rotating massive star. Compared to time-averaged MHD simulations, this analytic prescription provides a satisfactory description of magnetospheres, and can be used to synthesize various diagnostics (e.g. Hα and optical photometric measurements; Owocki et al 2016; Munoz et al 2020), as well as the strong, wind-sensitive lines found in the ultraviolet (Hennicker et al, 2018; Erba et al, 2021a).

Figure 5 shows that when coupled with appropriate radiative transfer techniques, UV line profiles synthesized using the ADM formalism generally compare well with those produced using an MHD magnetosphere.

The ADM model relies on a few simplifying assumptions: rotation is not taken into account, the dynamic flows formed by alternating episodes of wind launching and infall back onto the stellar surface are approximated by using an unphysical superposition of an upflow and a downflow component, and the magnetic field is idealized as a pure dipole. The latter assumption can be relaxed to take into account various values of $R_{\rm A}$ (e.g. Erba et al 2021a), and even an arbitrary magnetic geometry (Fletcher et al, 2017).

Given its success in reproducing a range of observational diagnostics, the ADM model represents a computationally inexpensive alternative to MHD simulations, especially given the wide
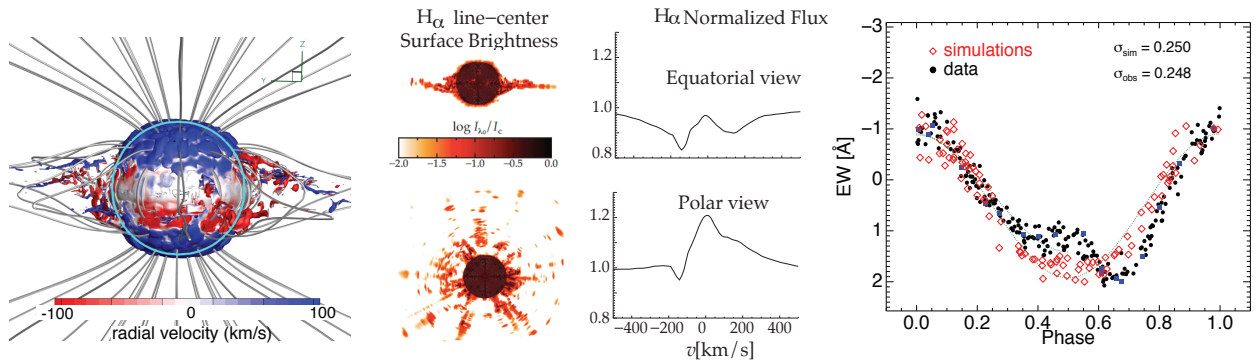
Fig. 4 3D MHD model of the dynamical magnetosphere for the young, slowly rotating (15.4-day period) O7V star θ^1 Ori C. The left panel shows a snapshot of wind structure drawn as isodensity surface, colored to show radial component of velocity. The middle panels shows the predicted equatorial and polar views of Hα line-center surface brightness, along with corresponding line-flux profiles. The right panel compares the observed rotational modulation of the Hα equivalent width (black) with 3D model predictions (red) assuming a pure-dipole surface field tilted by $\beta = 45°$ to the rotation axis, as viewed from the inferred observer inclination of $i = 45°$. Figure adopted from ud-Doula et al (2013).

parameter space probed in UV studies of magnetospheres. Erba et al (2021a) developed a grid of synthetic UV line profiles using the ADM formalism coupled with a simplified radiative transfer technique (using their *UV-ADM* code). They reported the first large-scale parameter study of several factors (e.g. magnetosphere size, line strength, observer's viewing angle) that affect UV wind line formation, with model parameters chosen to correspond with specific magnetic massive stars (e.g. HD 191612, NGC 1624-2).

The application of the ADM model to UV spectral line synthesis by Erba et al (2021a) has also provided evidence for spectral features in the ultraviolet that appear to be unique to magnetic massive stars, including the presence of red-shifted absorption and a strong desaturation of the high-velocity absorption trough, resulting in a spectrum which appears to be of a later type than would be assumed from other observations (e.g. optical). Such signatures could help establish ultraviolet spectroscopy as a means of indirectly detecting magnetic fields in massive stars, similarly to other rotationally-modulated variations across the electromagnetic spectrum (e.g. optical photometric variations, Hα emission, or gyrosynchrotron radio emission David-Uraz et al, 2019b; Shultz et al, 2020; Leto et al, 2021). Of particular interest to Polstar, the red-shifted absorption feature is a diagnostic of infalling plasma (Erba et al, 2021a). As can be seen in the lower panel of

Fig. 5, which compares synthetic UV line profiles computed using an ADM (solid lines) versus an MHD (dashed lines) magnetospheric model, red-shifted absorption in the line profile is a subtle feature in the total line profile (see Figures 5-6 of Erba et al, 2021a, for a more detailed description of the red-shifted absorption feature). Detection of such infalling material using e.g. Polstar will require high S/N and high spectral resoluton.

3 Linear spectropolarimetry in the UV

The basic idea of linear spectropolarimetry is rather straightforward: electrons in an extended circumstellar medium scatter radiation from the stellar surface, giving rise to a certain linear polarization level. If the sky-projected electron distribution is perfectly circular, the linear Stokes Q and U vectors cancel, and linear polarization remains absent. If the geometry is not circular, but an asymmetry is involved, this results in some level of continuum linear polarization of order 1% (e.g. Harries et al, 2002).

One of the advantages of linear spectropolarimetry over continuum polarimetry is that it is possible to perform differential measurements between a line and the continuum – independent of interstellar and /or instrumental polarization. One example may occur across an emission line. This
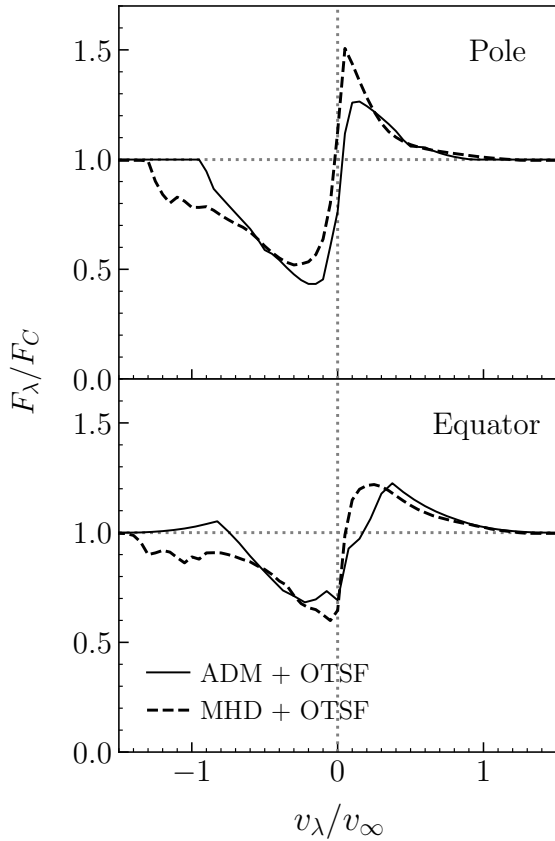
Fig. 5 Two sets of synthetic UV line profiles are compared for a magnetic pole-on (upper panel) and equator-on (lower panel) view. The first set of models (solid lines) calculates the density and velocity structure of the magnetosphere using the ADM formalism (Erba et al, 2021a) and model parameters similar to the star θ^1 Ori C (R_A = 2.3 R_*, v_∞ = 3200 km s^{-1}) ; the second set (dashed lines) is calculated using a snapshot of the 3D MHD magnetosphere generated for θ^1 Ori C (ud-Doula et al, 2013). To produce the line profiles, both sets of models are coupled with the same radiative transfer method that employs the optically thin source function (OTSF). Overall, the line profiles from these two model sets have similar characteristic shapes.

"line effect" relies on the expectation that recombination lines arise over a much larger volume than the continuum, and becomes *de*polarized (see the left hand side of Fig. 6). Depolarization immediately indicates the presence or absence of asphericity.

The bulk of linear spectropolarimetric studies involved these depolarization line effects, but in some situations there is evidence for intrinsic *line* polarization, such as was predicted by Wood et al (1993) and found observationally in pre-main

sequence T Tauri and Herbig Ae/Be stars (Vink et al, 2002, 2005b). In such cases the line photons are assumed to originate from a more compact source (e.g. as a result of magnetospheric phenomena), and these photons are scattered off a rotating disk, leading to a flip in the position angle (PA), resulting in a rounded loop (rather than a linear excursion) in the QU diagram (sketched on the right hand side of Fig, 6).
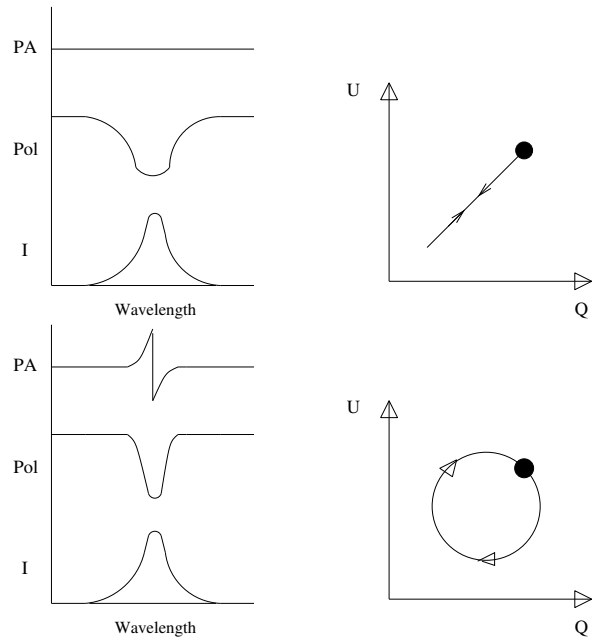

Fig. 6 Cartoons representing line *depolarization* (top row) and compact line emission scattered off a rotating disk (bottom row) as triplots and QU diagrams. Stokes I profiles are plotted in the lower triplot panels, % Pol in the middle panels, and the position angles (PAs) are shown in the upper triplot panels. Line depolarization is as broad as the Stokes I emission, while *line* polarization is narrow by comparison. Depolarization translates into QU space as a linear excursion, while *line* polarization PA flips are associated with QU loops.

Motivated by the high incidence of QU loops in T Tauri and Herbig Ae stars, Vink et al (2005a) developed Monte Carlo polarization models of scattering off rotating disks – with and without inner holes. Figure 7 shows a pronounced difference between scattering off a disk that hits the stellar surface (right-hand side), and one with a sizeable inner hole (left-hand side). The single PA flips on the left are similar to those predicted analytically (Wood et al, 1993), but the double PA flips on the right – associated with undisrupted

disks – have only been found numerically. They are thought to be unique to the appropriate geometric treatment of a finite-sized star that interacts with the velocity structure of the disk.

The numerical models demonstrate the potential of instrinsic line polarimetry to determine not only disk inclination, but also the physical sizes of the inner regions associated with magnetospheres. Linear line polarimetry is so far the only method capable of doing this on such small spatial scales, within just a few stellar radii from the stellar surface.
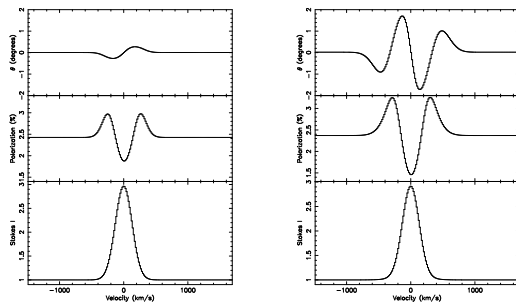
Fig. 7 Monte Carlo line polarimetry for the case of a disk with an inner hole (left hand side) and without an inner hole – a result of the finite size of the star (right hand side) (Vink et al, 2005b).

Several studies of linearly polarized Hα emission have been conducted for AGB, T Tauri, and Herbig Ae/Be stars by Vink et al (2005a), Harrington and Kuhn (2007, 2009), and Ababakr et al (2016, 2017). These have found line polarization amplitudes of order 0.1-1%, detectable at an unbinned S/N of $\sim 200-1000$. This is comparable to the S/N required for circumstellar magnetometry, therefore the same data that will enable the measurement of circumstellar magnetic fields should also enable the detection of circumstellar line polarization effects.

4 Continuum linear polarimetry in the UV

The presence of an obliquely rotating magnetosphere is largely responsible for the periodic modulation of the observable quantities of magnetic massive stars. As the star rotates, its own magnetosphere periodically occults the source star's light. For hot stars with winds primarily dominated by the electron scattering opacity, the bulk of their photometric and polarimetric variability can be estimated under the single-electron scattering approximation. In this case, the photometric variability is determined by the column density, while the polarimetric variability is characterised by the general shape of the magnetosphere.

Broadband linear polarimetry of stellar magnetospheres is observationally challenging: the typical levels of polarization are quite low, of order $10^{-4} - 10^{-3}$ (e.g. Carciofi et al, 2013; Munoz et al, 2020, , and Munoz et al. (accepted)). As a consequence, accurate monitoring of magnetospheric polarization on the relevant rotational timescales (ranging from days to years) requires understanding and eliminating competing instrumental effects.

Even in the optical, few studies of magnetospheric linear polarization have been carried out. The first such studies investigated the Centrifugal Magnetosphere of the archetypical He-strong Bp star σ Ori E by Kemp and Herman (1977) and Carciofi et al (2013). As shown in Fig. 8, Carciofi et al. obtained dense polarimetric coverage of the star's 1.19-day rotational cycle, measuring both the Q and U Stokes parameters with a typical precision of 10^{-4} (0.01%, about an order of magnitude better than in the pioneering study by Kemp and Herman 1977). They attempted to reproduce the observed polarimetric variations by feeding the density distribution for σ Ori E computed using the Rigidly Rotating Magnetosphere (RRM) model into a radiative transfer code. They were unable to find a model capable of simultaneously fitting both the photometry and the polarimetry, noting that a higher density model (solid line in Fig. 8) that matched the depth of the photometric eclipses predicted a polarization amplitude much larger than observed, while a lower-density model (dashed line in Fig. 8) that reproduced the amplitude of the polarization failed to reproduce the photometric amplitude. They were able to resolve these descripancies using an ad hoc "dumbbell + disc" model with a density distribution motivated by the RRM predictions. This study serves as an excellent illustration of the power of polarization to test theoretical models of magnetospheric density and geometry.

More recently, Munoz et al (2020) and Munoz et al. (accepted) have developed a capability to compute magnetospheric polarization in the framework of the ADM model (Fig. 9). Under the assumption of single electron scattering, they examined the behaviour of Stokes Q and U with changing magnetospheric (field strength and geometry) and stellar (mass, radius, and wind) properties. They demonstrated that linear polarization is uniquely able to disentangle the angular parameters i and β describing the magnetic geometry. They applied their model to the magnetic O star HD 191612, obtaining a self-consistent solution to the magnetic and stellar parameters capable of simultaneously reproducing the polarimetric measurements and Hipparcos photometry.

Today, high precision broadband polarization measurements are available for only a handful of magnetic stars. The potential of Polstar to collect similar data for a significant fraction of the population of known magnetic objects is extremely exciting, as it will accurate determination of their magnetic and wind parameters, and provide a broad parameteric basis for testing of the assumptions underpinning magnetospheric models. From the models and observations that have so far been published, polarization amplitudes of the order of 0.01% to 0.1% are expected (Carciofi et al, 2013; Munoz et al, 2020).

5 Enabled Science

Massive OB stars show variability both spectroscopically and photometrically in many wavelength bands including the UV, optical and X-ray. Regular variability could be related to stellar pulsations, rotation modulation, and/or the presence of globally organized magnetic fields, while widespread stochastic variability on hourly to daily timescales is poorly understood. Stochastic variability could be caused by the presence of bright spots (possibly of magnetic origin), clumps, internal gravity waves (Bowman et al, 2019, 2020), or subsurface convection (Cantiello et al, 2021). A well-known example of irregular variability in UV wind-line profiles are discrete absorption components (DACs). The formation of these wind structures are ascribed to corotating interacting regions (CIRs, Mullan 1984, 1986), which arise above bright spots at the stellar surface (Cranmer and Owocki, 1996). The formation of bright

surface spots can be caused by magnetic fields produced by dynamo action in the subsurface convection layer and brought up to the surface by buoyancy (Cantiello and Braithwaite, 2011). The lifetime of these fields is determined by the relatively short turnover time of the subsurface layer. The expected strength of these fields imply the local magnetic confinement parameter to be around unity (ud-Doula and Owocki, 2002) i.e. the fields are able affect the wind dynamically.

The small-scale magnetic fields that appear at the surface as bright spots can be a driver of many surface related phenomena observed in OB stars. Short-lived bright spots give rise to low-amplitude ($\simeq$ 10 mmag) photometric variability, as observed by space-based high-precision photometry (MOST, BRITE, TESS) in the light curves of many OB stars. Ramiaramanantsoa et al (2014) simulated the MOST light curve of the O7.5 III(n)((f)) star ξ Per with several corotating bright spots, presumably of magnetic origin, with random starting times and lifetimes up to several rotations varying from one spot to another. Analysing simultaneous photometry from the BRITE constellation and ground-based spectroscopy for the O4I(n)fp star ζ Pup, Ramiaramanantsoa et al (2018) established an empirical link between wind structures and photospheric activity, implying a photospheric origin. Two types of variability were found: one single-periodic non-sinusoidal component with 1.78 d period, superimposed on a stochastic component. The periodic component is consistent with rotational modulation arising from evolving bright spots that were mapped at the surface. The signal was also found in the He II λ4686 wind emission line, showing signatures of corotating interaction regions that turn out to be driven by the bright photospheric spots observed by BRITE. The spots are suggested to originate from small-scale magnetic fields generated through dynamo action within a subsurface convection zone (e.g. Cantiello and Braithwaite, 2011; Jermyn and Cantiello, 2020). The stochastic component observed in He II λ4686 line correlated with the amplitudes of stochastic light variations. Stochastic He II variability was attributed to wind clumps, while stochastic photometric variability was proposed to be the photospheric drivers of the clumps.

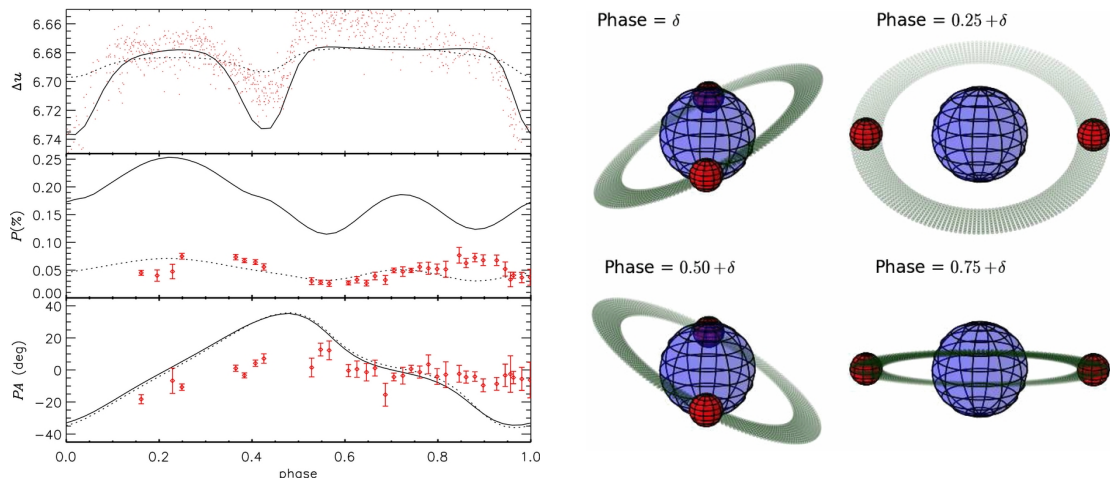David-Uraz et al (2017) investigated whether bright spots compatible with recent observation

Fig. 8 *Left:* Modeling of the intrinsic polarization of σ Ori E using the RRM model (observations are in red). The only free parameter is the maximum number density in the magnetosphere, which was set to 10^{12} cm^{-3} (solid lines) to reproduce the depth of the eclipses and 2.5×10^{11} cm^{-3} (dotted lines) to reproduce the amplitude of the linear polarization. *Right:* Geometric conception of the "dumbbell + disk" model to scale. From Carciofi et al (2013).

could be responsible for DACs observed in the UV line profiles of the O7.5 III(n)((f)) star ξ Per. The authors successfully reproduced the behaviour of DACs with 4 equally spaced equatorial spots with angular radius $10°$ and $20°$. In this scenario spots appearing and disappearing randomly over time, with varying strengths and sizes, might explain the cyclical nature of DACs. Semi-analytic analysis for the spot size and amplitude needed to produce an overloaded wind that form the DAC was done by Owocki (2018).

Unexpectedly, the signature of DACs has been detected in the X-ray range (ζ Pup - Nazé et al 2018; Nichols et al 2021, λ Cep - Rauw et al 2015, ξ Per - Massa et al 2019). Their presence and characteristics were not predicted by current models. UV data can however constrain in detail the spots and wind structures, leading to better modelling and a full understanding of these high-energy features.

Based on spectroscopic analysis of the He II $\lambda4686$ line for the O6I(n)fp star λ Cep, it was proposed that cyclical variations are caused by the presence of multiple, transient, short-lived, corotating magnetic loops – so-called *stellar prominences* – likely associated with bright surface spots (Sudnik and Henrichs, 2016). The prominences are represented as corotating spherical blobs of emitting gas attached to the surface of the star. Depending on its location, the blob contributes

to the line profile as an emission or absorption feature.

An example of the model fit of subsequent quotient spectra i.e., the following spectrum divided by the previous one, is shown in Fig. 10. The proposed model applied to the He II $\lambda4686$ line can be fitted with 2-5 equatorial blobs with lifetimes between $\sim$1 and 24 h. The action of the subsurface convection zone would be the most likely driving mechanism that generates short-lived magnetic bright spots as the source of prominences.

Local small scale magnetic fields tied to stellar prominences can be viewed as an off-center small (tiny) dipole with its center located close to the stellar surface. Such small scale fields can cause variability at the stellar surface that can propagate outwards affecting what is observed in these winds. As a proof-of-concept, we have carried out some preliminary 3D MHD simulations of hot star winds wherein we assumed that the location of the strong local field coincides with bright spots using the approach of Owocki (2018). Fig. 11 shows the logarithmic density of two such sample models for a typical hot star viewed along ZX-plane. The left panel shows a case where the small scale dipole field is aligned with rotation axis, and the right panel has an inclination angle of $90°$ with respect to the rotational axis. We assumed rotation of 0.5 critical, and a field strength of order kG at the stellar surface that falls off steeply with distance from the photosphere. As seen in Fig. 11, despite being
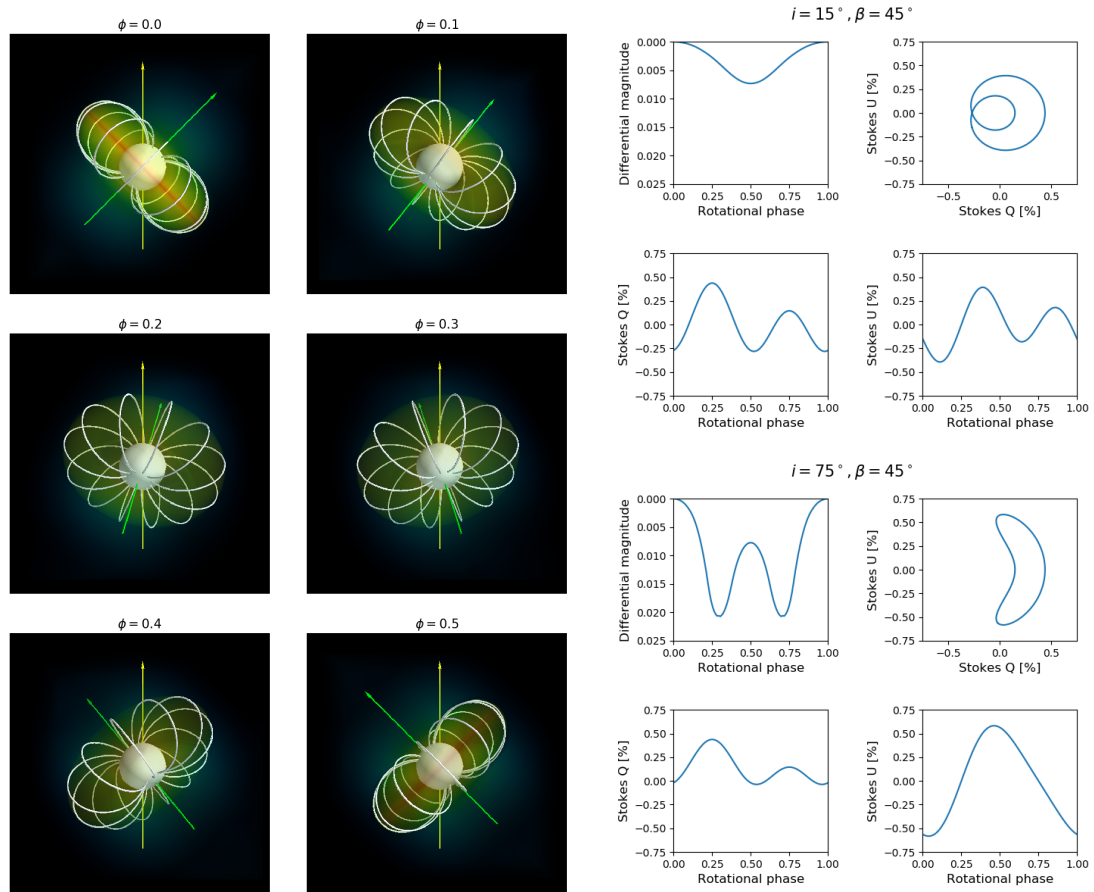
Fig. 9 *Left:* Illustration of the density field of the Analytic Dynamical Magnetosphere (ADM) model at 6 rotational phases. *Right:* Photometric and polarimetric phase variations predicted for ADM models having two different geometries ($i = 15°$, $\beta = 45°$ (top), $i = 75°$, $\beta = 45°$ (bottom)). From Munoz et al (2020).

localized, this field can substantially influence the wind dynamics globally.

While such small-scale fields cannot be detected with existing ground-based facilities, ultraviolet spectropolarimetry may provide an avenue for direct detection, for instance via the Hanle effect (if they are relatively weak), or even via the Zeeman effect (if the spots are large, the field strong, with an advantage being gained by the greater brightness of the spots in the UV). Linear spectropolarimetry will further provide important geometrical data that may help distinguish between CIR models with and without magnetic fields.

6 Summary

In this paper we have described how the unique capabilities offered by Polstar will lead to fundamental advances in our understanding of the magnetospheres of hot stars. While the focus of this paper has been on the capabilities of the Polstar mission, this work is of relevance to any ultraviolet spectropolarimetric mission, such as Arago.

The high-resolution ultraviolet spectra obtained by Polstar will enable much more precise spectroscopic evaluation of stellar magnetospheres, as compared to the lower-resolution, lower-S/N data available for most stars via the Interstellar Ultraviolet Explorer. Importantly, over half of the non-magnetic stars proposed to be observed by Polstar do not have a single UV
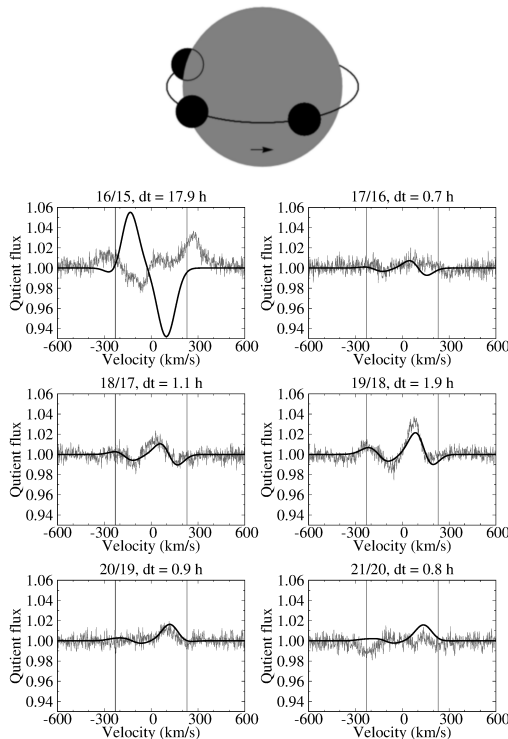
Fig. 10 Model fits (black thick lines) for subsequent quotient spectra of He II λ4686 line for the star λ Cep (gray thin lines) of the 2013 dataset, spectra 15–21. The top label gives the sequence numbers of the two spectra of the quotient, followed by their time interval in hours. The geometry which is depicted at the beginning of the series, is used for all figures in the sequence and shown for the epoch of the first spectrum in the series. The star rotates but the blobs keep their same relative position. The first and last figure of the series contains intentionally failed fits, to signify the extend over which the fitted configuration, carried around by the rotation, survives (Sudnik and Henrichs, 2016).

observation; of those that do, only a small fraction have time-series data adequate for evaluation of the projected magnetospheric geometry and column density across a rotational cycle.

While surface magnetic field measurements obtained via ground-based visible spectropolarimetry are already available for all stars in the sample, the large number of spectral lines available for multi-line analysis in high-resolution ultraviolet spectra more than compensates for the weaker Zeeman effect at shorter wavelengths, in principle enabling higher-precision magnetic meeasurements to be obtained in the UV as compared to the visible. The full-Stokes capability of Polstar, and expected advantages in the UV over

the visible in the amplitude of Stokes QU signals associated with the transverse Zeeman effect, mean that many of the datasets will be optimal for magnetic mapping via full-Stokes Zeeman Doppler Imaging (ZDI). Importantly, the availability of all four Stokes parameters for magnetic inversion breaks degeneracies that can affect maps obtained only in Stokes IV.

Polstar will enable measurement of circumstellar magnetic fields, with the projected capabilities of the instrument capable of detecting magnetic signatures originating in the circumstellar environment in a large fraction of known magnetic stars. Strong fields should be detectable via the Zeeman effect (as evaluated using state of the art magnetospheric models).

Both high- and low- resolution linear spectropolarimetry will provide crucial and sensitive constraints on the magnetospheric geometry, enabling degeneracies between rotational axis inclinations and magnetic axis tilt angles to be broken. Importantly, the information available via linear polarization provides geometrical data that cannot be obtained via spectroscopy or photometry alone, as already revealed by the insufficiency of current magnetospheric models to simultaneously reproduce the light curve and polarimetric variation of σ Ori E.

By combining the rich spectroscopic and polarimetric datasets available with Polstar observations, detailed 3D models of the circumstellar environments of a large number of magnetic hot stars can be compared against constraints on the circumstellar magnetic field, column density, velocity structure, and geometry. This will enable measurement of the escaping and magnetically trapped wind fraction of these stars across a full range of stellar, evolutionary, magnetic, and rotational parameters, thereby providing a crucial test of the expectation that magnetic fields rapidly drain angular momentum and drastically reduce the net mass-loss rates of massive stars. This will provide empirical calibration for evolutionary models incorporating rotation and magnetic fields, which will in turn provide important information for the stellar population synthesis models used to infer the mass and energy budget for the interstellar medium, expectations for the properties of post-main sequence supergiants and supernovae, and the population statistics of stellar remnants.
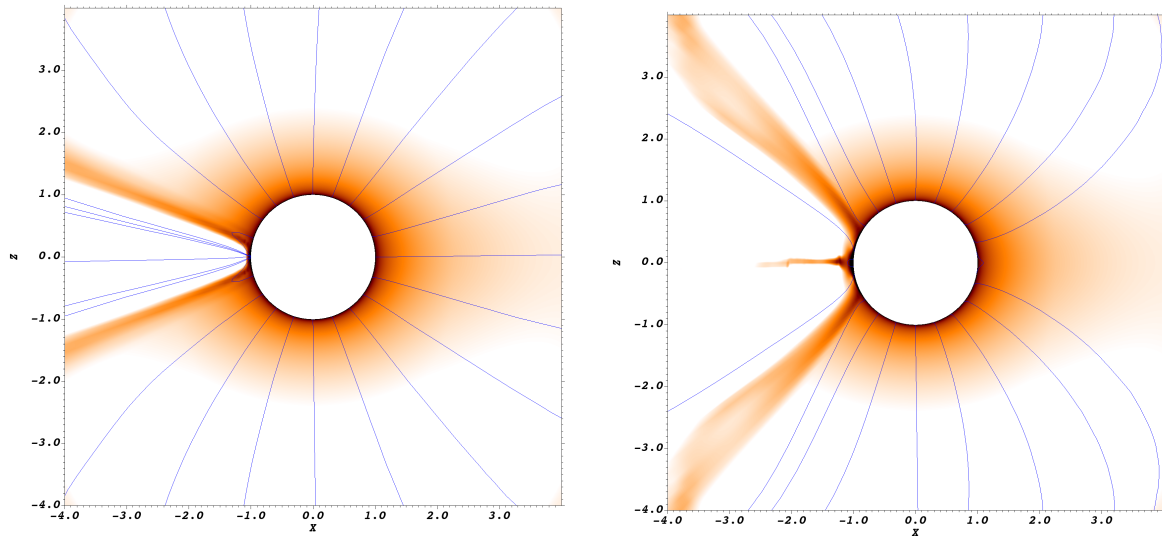
Fig. 11 Logarithm of density of ZX-plane of 3D MHD simulations of a sample O-star wind with a small scale off-center magnetic dipole field to mimic small scale strong magnetic field that can perturb the wind at the base. The angle between rotation ($W = 0.5$ half critical) and magnetic axes $\beta = 0°$ (*left panel*) and $\beta = 90°$ (*right panel*). The color code represents the logarithm of density in a range 10^{-15} to 10^{-11} g/cm^3. Blue lines represent time-evolved magnetic field lines which are strong only over limited area on the stellar surface and fall of steeply with distance away from the star.

References

Ababakr KM, Oudmaijer RD, Vink JS (2016) Linear spectropolarimetry across the optical spectrum of Herbig Ae/Be stars. $MNRAS$461(3):3089–3110. https://doi.org/10.1093/mnras/stw1534, https://arxiv.org/abs/arXiv:1607.02440 [astro-ph.SR]

Ababakr KM, Oudmaijer RD, Vink JS (2017) A statistical spectropolarimetric study of Herbig Ae/Be stars. $MNRAS$472(1):854–868. https://doi.org/10.1093/mnras/stx1891, https://arxiv.org/abs/arXiv:1707.08408 [astro-ph.SR]

Abt HA, Levato H (1977) Spectral types in the Orion OB1 association. PASP89:797–802. https://doi.org/10.1086/130230

Adams FC, Laughlin G (1997) A dying universe: the long-term fate and evolutionof astrophysical objects. Reviews of Modern Physics 69(2):337–372. https://doi.org/10.1103/RevModPhys.69.337, https://arxiv.org/abs/arXiv:astro-ph/9701131 [astro-ph]

Babel J, Montmerle T (1997) X-ray emission from Ap-Bp stars: a magnetically confined wind-shock model for IQ Aur. A&A323:121–138

Berghoefer TW, Schmitt JHMM, Cassinelli JP (1996) The ROSAT all-sky survey catalogue of optically bright OB-type stars. A&AS118:481–494

Blazère A, Petit P, Neiner C, et al (2020) Magnetic geometry and surface differential rotation of the bright Am star Alhena A. $MNRAS$492(4):5794–5810. https://doi.org/10.1093/mnras/stz3637, https://arxiv.org/abs/arXiv:1912.08688 [astro-ph.SR]

Bowman DM, Burssens S, Pedersen MG, et al (2019) Low-frequency gravity waves in blue supergiants revealed by high-precision space photometry. Nature Astronomy 3:760–765. https://doi.org/10.1038/s41550-019-0768-1, https://arxiv.org/abs/arXiv:1905.02120 [astro-ph.SR]

Bowman DM, Burssens S, Simón-Díaz S, et al (2020) Photometric detection of internal gravity waves in upper main-sequence

stars. II. Combined TESS photometry and high-resolution spectroscopy. A&A640:A36. https://doi.org/10.1051/0004-6361/202038224, https://arxiv.org/abs/arXiv:2006.03012 [astro-ph.SR]

Braithwaite J, Spruit HC (2004) A fossil origin for the magnetic field in A stars and white dwarfs. Nature431:819–821. https://doi.org/10.1038/nature02934, https://arxiv.org/abs/0502043

Brott I, de Mink SE, Cantiello M, et al (2011) Rotating massive main-sequence stars. I. Grids of evolutionary models and isochrones. A&A530:A115. https://doi.org/10.1051/0004-6361/201016113, https://arxiv.org/abs/arXiv:1102.0530 [astro-ph.SR]

Cantiello M, Braithwaite J (2011) Magnetic spots on hot massive stars. A&A534:A140. https://doi.org/10.1051/0004-6361/201117512, https://arxiv.org/abs/arXiv:1108.2030 [astro-ph.SR]

Cantiello M, Lecoanet D, Jermyn AS, et al (2021) On the Origin of Stochastic, Low-Frequency Photometric Variability in Massive Stars. ApJ915(2):112. https://doi.org/10.3847/1538-4357/ac03b0

Carciofi AC, Faes DM, Townsend RHD, et al (2013) Polarimetric Observations of σ Orionis E. $ApJL$766(1):L9. https://doi.org/10.1088/2041-8205/766/1/L9, https://arxiv.org/abs/arXiv:1302.4684 [astro-ph.SR]

Carneiro LP, Puls J, Sundqvist JO, et al (2016) Atmospheric NLTE models for the spectroscopic analysis of blue stars with winds. III. X-ray emission from wind-embedded shocks. A&A590:A88. https://doi.org/10.1051/0004-6361/201527718, https://arxiv.org/abs/arXiv:1603.01177 [astro-ph.SR]

Chandra P, Wade GA, Sundqvist JO, et al (2015) Detection of 610-MHz radio emission from hot magnetic stars. $MNRAS$452(2):1245–1253. https://doi.org/10.1093/mnras/stv1378,

https://arxiv.org/abs/arXiv:1505.02139 [astro-ph.SR]

Cheung MCM, De Pontieu B, Tarbell TD, et al (2015) Homologous Helical Jets: Observations By IRIS, SDO, and Hinode and Magnetic Modeling With Data-Driven Simulations. ApJ801(2):83. https://doi.org/10.1088/0004-637X/801/2/83, https://arxiv.org/abs/arXiv:1501.01593 [astro-ph.SR]

Cosentino G, Jiménez-Serra I, Tan JC, et al (2022) Negative and positive feedback from a supernova remnant with SHREC: a detailed study of the shocked gas in IC443. $MNRAS$511(1):953–963. https://doi.org/10.1093/mnras/stac070, https://arxiv.org/abs/arXiv:2201.03008 [astro-ph.GA]

Cranmer SR, Owocki SP (1996) Hydrodynamical Simulations of Corotating Interaction Regions and Discrete Absorption Components in Rotating O-Star Winds. ApJ462:469

Das B, Chandra P, Shultz ME, et al (2021) Discovery of eight 'Main-sequence Radio Pulse emitters' using the GMRT: clues to the onset of coherent radio emission in hot magnetic stars. arXiv e-prints arXiv:2109.04043. https://arxiv.org/abs/arXiv:2109.04043 [astro-ph.SR]

David-Uraz A, Owocki SP, Wade GA, et al (2017) Investigating the origin of cyclical wind variability in hot massive stars - II. Hydrodynamical simulations of corotating interaction regions using realistic spot parameters for the O giant ξ Persei. $MNRAS$470(3):3672–3684. https://doi.org/10.1093/mnras/stx1478, https://arxiv.org/abs/arXiv:1706.03647 [astro-ph.SR]

David-Uraz A, Erba C, Petit V, et al (2019a) Extreme resonance line profile variations in the ultraviolet spectra of NGC 1624-2: probing the giant magnetosphere of the most strongly magnetized known O-type star. $MNRAS$483(2):2814–2824. https://doi.org/10.1093/mnras/sty3227, https://arxiv.org/abs/arXiv:1811.10113 [astro-ph.SR]

David-Uraz A, Neiner C, Sikora J, et al (2019b) Magnetic OB[A] Stars with TESS: probing their Evolutionary and Rotational properties (MOBSTER) - I. First-light observations of known magnetic B and A stars. $MNRAS$487(1):304–317. https://doi.org/10.1093/mnras/stz1181, https://arxiv.org/abs/arXiv:1904.11539 [astro-ph.SR]

David-Uraz A, Petit V, Shultz ME, et al (2021) New observations of NGC 1624-2 reveal a complex magnetospheric structure and underlying surface magnetic geometry. $MNRAS$501(2):2677–2687. https://doi.org/10.1093/mnras/staa3768, https://arxiv.org/abs/arXiv:2010.07482 [astro-ph.SR]

Donati JF, Landstreet JD (2009) Magnetic Fields of Nondegenerate Stars. ARAA47(1):333–370. https://doi.org/10.1146/annurev-astro-082708-101833, https://arxiv.org/abs/arXiv:0904.1938 [astro-ph.SR]

Donati JF, Howarth ID, Jardine MM, et al (2006a) The surprising magnetic topology of τ Sco: fossil remnant or dynamo output? $MNRAS$370(2):629–644. https://doi.org/10.1111/j.1365-2966.2006.10558.x, https://arxiv.org/abs/arXiv:astro-ph/0606156 [astro-ph]

Donati JF, Howarth ID, Jardine MM, et al (2006b) The surprising magnetic topology of τ Sco: fossil remnant or dynamo output? $MNRAS$370(2):629–644. https://doi.org/10.1111/j.1365-2966.2006.10558.x, https://arxiv.org/abs/arXiv:astro-ph/0606156 [astro-ph]

Driessen FA, Kee ND, Sundqvist JO (2021) Simulations of the line-driven instability in magnetic hot star winds. arXiv e-prints arXiv:2110.05302. https://arxiv.org/abs/arXiv:2110.05302 [astro-ph.SR]

Erba C, David-Uraz A, Petit V, et al (2021a) Ultraviolet line profiles of slowly rotating massive star winds using the 'analytic dynamical magnetosphere' formalism. $MNRAS$506(4):5373–5388.

https://doi.org/10.1093/mnras/stab1853, https://arxiv.org/abs/arXiv:2106.13676 [astro-ph.SR]

Erba C, Shultz ME, Petit V, et al (2021b) Confirmation of ξ^1 CMa's ultra-slow rotation: magnetic polarity reversal and a dramatic change in magnetospheric UV emission lines. $MNRAS$506(2):2296–2308. https://doi.org/10.1093/mnras/stab1454, https://arxiv.org/abs/arXiv:2105.08192 [astro-ph.SR]

Favata F, Neiner C, Testa P, et al (2009) Testing magnetically confined wind shock models for β Cephei using XMM-Newton and Chandra phase-resolved X-ray observations. A&A495(1):217–229. https://doi.org/10.1051/0004-6361:20078529, https://arxiv.org/abs/arXiv:0806.2275 [astro-ph]

Feldmeier A, Puls J, Pauldrach AWA (1997) A possible origin for X-rays from O stars. A&A322:878–895

Fletcher CL, Petit V, Nazé Y, et al (2017) Investigating the Magnetospheres of Rapidly Rotating B-type Stars. In: Eldridge JJ, Bray JC, McClelland LAS, et al (eds) The Lives and Death-Throes of Massive Stars, pp 369–372, https://doi.org/10.1017/S1743921317002812, 1702.06500

Fletcher CL, Petit V, Cohen DH, et al (2018) Detailed ADM-based Modeling of Shock Retreat and X-ray Emission of τ Sco. Contributions of the Astronomical Observatory Skalnate Pleso 48(1):144–148

Folsom CP, Petit P, Bouvier J, et al (2016) The evolution of surface magnetic fields in young solar-type stars - I. The first 250 Myr. $MNRAS$457:580–607. https://doi.org/10.1093/mnras/stv2924, https://arxiv.org/abs/arXiv:1601.00684 [astro-ph.SR]

Gagné M, Oksala ME, Cohen DH, et al (2005) Chandra HETGS Multiphase Spectroscopy of the Young Magnetic

O Star θ^1 Orionis C. *ApJ*628(2):986–1005. https://doi.org/10.1086/430873, https://arxiv.org/abs/arXiv:astro-ph/0504296 [astro-ph]

Grudić MY, Guszejnov D, Offner SSR, et al (2022) The dynamics and outcome of star formation with jets, radiation, winds, and supernovae in concert. *MNRAS*512(1):216–232. https://doi.org/10.1093/mnras/stac526, https://arxiv.org/abs/arXiv:2201.00882 [astro-ph.GA]

Grunhut JH, Wade GA, Marcolino WLF, et al (2009) Discovery of a magnetic field in the O9 sub-giant star HD 57682 by the MiMeS Collaboration. *MNRAS*400(1):L94–L98. https://doi.org/10.1111/j.1745-3933.2009.00771.x, https://arxiv.org/abs/arXiv:0910.0214 [astro-ph.SR]

Grunhut JH, Rivinius T, Wade GA, et al (2012) HR 5907: Discovery of the most rapidly rotating magnetic early B-type star by the MiMeS Collaboration. *MNRAS*419:1610–1627. https://doi.org/10.1111/j.1365-2966.2011.19824.x, https://arxiv.org/abs/arXiv:1109.3157 [astro-ph.SR]

Grunhut JH, Wade GA, Neiner C, et al (2017) The MiMeS survey of Magnetism in Massive Stars: magnetic analysis of the O-type stars. *MNRAS*465:2432–2470. https://doi.org/10.1093/mnras/stw2743, https://arxiv.org/abs/arXiv:1610.07895 [astro-ph.SR]

Harries TJ, Howarth ID, Evans CJ (2002) Spectropolarimetry of O supergiants. *MNRAS*337(1):341–355. https://doi.org/10.1046/j.1365-8711.2002.05926.x

Harrington DM, Kuhn JR (2007) Spectropolarimetry of the Hα Line in Herbig Ae/Be Stars. *ApJL*667(1):L89–L92. https://doi.org/10.1086/521999, https://arxiv.org/abs/arXiv:0708.0601 [astro-ph]

Harrington DM, Kuhn JR (2009) Spectropolarimetric Observations of Herbig Ae/Be Stars. II. Comparison of Spectropolarimetric Surveys: Haebe, Be and Other Emission-Line Stars. ApJS180(1):138–181. https://doi.org/10.1088/0067-0049/180/1/138, https://arxiv.org/abs/arXiv:0809.3849 [astro-ph]

Hennicker L, Puls J, Kee ND, et al (2018) 3D radiative transfer: Continuum and line scattering in non-spherical winds from OB stars. A&A616:A140. https://doi.org/10.1051/0004-6361/201731858, https://arxiv.org/abs/arXiv:1806.08155 [astro-ph.SR]

Henrichs HF (2001) Magnetic Fields in Hot Stars: Indirect Indicators. In: Mathys G, Solanki SK, Wickramasinghe DT (eds) Magnetic Fields Across the Hertzsprung-Russell Diagram, p 393

Henrichs HF, Kolenberg K, Plaggenborg B, et al (2012) Discovery of a magnetic field in the early B-type star σ Lupi. A&A545:A119. https://doi.org/10.1051/0004-6361/201219632, https://arxiv.org/abs/arXiv:1208.4627 [astro-ph.SR]

Henrichs HF, de Jong JA, Verdugo E, et al (2013) Discovery of the magnetic field in the pulsating B star β Cephei. A&A555:A46. https://doi.org/10.1051/0004-6361/201321584, https://arxiv.org/abs/arXiv:1305.2601 [astro-ph.SR]

Jermyn AS, Cantiello M (2020) The Origin of the Bimodal Distribution of Magnetic Fields in Early-type Stars. *ApJ*900(2):113. https://doi.org/10.3847/1538-4357/ab9e70, https://arxiv.org/abs/arXiv:2006.08618 [astro-ph.SR]

Jermyn AS, Cantiello M (2021) Magnetic Archaeology of Early-Type Stellar Dynamos. arXiv e-prints arXiv:2110.03695. https://arxiv.org/abs/arXiv:2110.03695 [astro-ph.SR]

Johnson JA (2019) Populating the periodic table: Nucleosynthesis of the elements. Science 363(6426):474–478. https://doi.org/10.1126/science.aau9540, URL https://www.science.org/doi/abs/10.1126/science.aau9540,

https://arxiv.org/abs/https://www.science.org/doi/pdf/10.1126/science.au9540

Kemp JC, Herman LC (1977) The polarization of Sigma Orionis E, a curious eclipsing binary. *ApJ*218:770–775. https://doi.org/10.1086/155733

Kochukhov O, Shultz M, Neiner C (2019) Magnetic field topologies of the bright, weak-field Ap stars θ Aurigae and ϵ Ursae Majoris. A&A621:A47. https://doi.org/10.1051/0004-6361/201834279, https://arxiv.org/abs/arXiv:1811.04928 [astro-ph.SR]

Leto P, Trigilio C, Krtička J, et al (2021) A scaling relationship for non-thermal radio emission from ordered magnetospheres: from the top of the main sequence to planets. *MNRAS*507(2):1979–1998. https://doi.org/10.1093/mnras/stab2168, https://arxiv.org/abs/arXiv:2107.11995 [astro-ph.SR]

Marcolino WLF, Bouret JC, Walborn NR, et al (2012) HST/STIS spectroscopy of the magnetic Of?p star HD 108: the low state at ultraviolet wavelengths. *MNRAS*422(3):2314–2321. https://doi.org/10.1111/j.1365-2966.2012.20820.x, https://arxiv.org/abs/arXiv:1202.6041 [astro-ph.SR]

Marcolino WLF, Bouret JC, Sundqvist JO, et al (2013) Phase-resolved ultraviolet spectroscopy of the magnetic Of?p star HD 191612. *MNRAS*431(3):2253–2260. https://doi.org/10.1093/mnras/stt323, https://arxiv.org/abs/arXiv:1302.4708 [astro-ph.SR]

Martin AJ, Neiner C, Oksala ME, et al (2018) First results from the LIFE project: discovery of two magnetic hot evolved stars. *MNRAS*475(2):1521–1536. https://doi.org/10.1093/mnras/stx3264, https://arxiv.org/abs/arXiv:1712.07403 [astro-ph.SR]

Martins F, Donati JF, Marcolino WLF, et al (2010) Detection of a magnetic field on HD108: clues to extreme braking and the Of?p phenomenon. *MNRAS*407(3):1423–1432. https://doi.org/10.1111/j.1365-2966.2010.17005.x, https://arxiv.org/abs/arXiv:1005.1854 [astro-ph.SR]

Massa D, Oskinova L, Prinja R, et al (2019) Coordinated UV and X-Ray Spectroscopic Observations of the O-type Giant ξ Per: The Connection between X-Rays and Large-scale Wind Structure. *ApJ*873(1):81. https://doi.org/10.3847/1538-4357/ab0283, https://arxiv.org/abs/arXiv:1901.09959 [astro-ph.SR]

Mewe R, Raassen AJJ, Cassinelli JP, et al (2003) High-resolution X-ray spectroscopy of tau Scorpii (B0.2V) with XMM-Newton. A&A398:203–211. https://doi.org/10.1051/0004-6361:20021577

Mullan DJ (1984) Corotating interaction regions in stellar winds. *ApJ*283:303–312

Mullan DJ (1986) Displaced narrow absorption components in the spectra of mass-losing OB stars - Indications of corotating interaction regions? A&A165:157–162

Munoz MS, Wade GA, Faes D, et al (2020) The Photometric and Polarimetric Variability of Magnetic O-type Stars. In: Wade G, Alecian E, Bohlender D, et al (eds) Stellar Magnetism: A Workshop in Honour of the Career and Contributions of John D. Landstreet, pp 148–155, 2004.13594

Nandra K, Barret D, Barcons X, et al (2013) The Hot and Energetic Universe: A White Paper presenting the science theme motivating the Athena+ mission. arXiv e-prints arXiv:1306.2307. https://arxiv.org/abs/arXiv:1306.2307 [astro-ph.HE]

Nazé Y, Rauw G, Pollock AMT, et al (2007) Towards an understanding of the Of?p star HD191612: phase-resolved multiwavelength observations. *MNRAS*375(1):145–153. https://doi.org/10.1111/j.1365-2966.2006.11270.x, https://arxiv.org/abs/arXiv:astro-ph/0611230 [astro-ph]

Nazé Y, Walborn NR, Rauw G, et al (2008) HD 148937: A Multiwavelength Study of the Third Galactic Member of the Of?p Class. *AJ*135(5):1946–1957. https://doi.org/10.1088/0004-6256/135/5/1946, https://arxiv.org/abs/arXiv:0803.0605 [astro-ph]

Nazé Y, ud-Doula A, Spano M, et al (2010) New findings on the prototypical Of?p stars. A&A520:A59. https://doi.org/10.1051/0004-6361/201014333, https://arxiv.org/abs/arXiv:1006.2054 [astro-ph.SR]

Nazé Y, Zhekov SA, Walborn NR (2012) High-resolution X-Ray Spectroscopy of the Magnetic Of?p Star HD 148937. *ApJ*746(2):142. https://doi.org/10.1088/0004-637X/746/2/142, https://arxiv.org/abs/arXiv:1111.7186 [astro-ph.SR]

Nazé Y, Petit V, Rinbrand M, et al (2014) X-Ray Emission from Magnetic Massive Stars. ApJS215:10. https://doi.org/10.1088/0067-0049/215/1/10, https://arxiv.org/abs/arXiv:1409.1690 [astro-ph.SR]

Nazé Y, Sundqvist JO, Fullerton AW, et al (2015) The changing UV and X-ray properties of the Of?p star CPD -28°2561. *MNRAS*452(3):2641–2653. https://doi.org/10.1093/mnras/stv1445, https://arxiv.org/abs/arXiv:1506.08572 [astro-ph.SR]

Nazé Y, ud-Doula A, Zhekov SA (2016) Chandra View of Magnetically Confined Wind in HD191612: Theory Versus Observations. *ApJ*831(2):138. https://doi.org/10.3847/0004-637X/831/2/138, https://arxiv.org/abs/arXiv:1608.08741 [astro-ph.SR]

Nazé Y, Ramiaramanantsoa T, Stevens IR, et al (2018) A detailed X-ray investigation of ζ Puppis. IV. Further characterization of the variability. A&A609:A81. https://doi.org/10.1051/0004-6361/201730729, https://arxiv.org/abs/arXiv:1710.09184 [astro-ph.HE]

Neiner C, Geers VC, Henrichs HF, et al (2003a) Discovery of a magnetic field in the Slowly Pulsating B star ¡ASTROBJ¿zeta Cassiopeiae¡/ASTROBJ¿. A&A406:1019–1031. https://doi.org/10.1051/0004-6361:20030742

Neiner C, Henrichs HF, Floquet M, et al (2003b) Rotation, pulsations and magnetic field in ¡ASTROBJ¿V 2052 Ophiuchi¡/ASTROBJ¿: A new He-strong star. A&A411:565–579. https://doi.org/10.1051/0004-6361:20031342

Neiner C, Oksala ME, Georgy C, et al (2017) Discovery of magnetic A supergiants: the descendants of magnetic main-sequence B stars. *MNRAS*471(2):1926–1935. https://doi.org/10.1093/mnras/stx1549, https://arxiv.org/abs/arXiv:1707.00560 [astro-ph.SR]

Nichols JS, Nazé Y, Huenemoerder DP, et al (2021) Correlated X-Ray and Optical Variability in the O-type Supergiant ζ Puppis. *ApJ*906(2):89. https://doi.org/10.3847/1538-4357/abca3a, https://arxiv.org/abs/arXiv:2011.07066 [astro-ph.HE]

Oksala ME, Grunhut JH, Kraus M, et al (2015a) An infrared diagnostic for magnetism in hot stars. A&A578:A112. https://doi.org/10.1051/0004-6361/201525987, https://arxiv.org/abs/arXiv:1505.01739 [astro-ph.SR]

Oksala ME, Kochukhov O, Krtička J, et al (2015b) Revisiting the rigidly rotating magnetosphere model for σ Ori E - II. Magnetic Doppler imaging, arbitrary field RRM, and light variability. *MNRAS*451(2):2015–2029. https://doi.org/10.1093/mnras/stv1086, https://arxiv.org/abs/arXiv:1505.04839 [astro-ph.SR]

Oksala ME, Neiner C, Wade G, et al (2021) New results of the LIFE project: characterization of the A5Ib-II supergiant 19 Aur and the newest sample of magnetic stars. In: MOBSTER-1 virtual conference: Stellar Variability as a Probe of Magnetic Fields in Massive Stars, p 47, https://doi.org/10.5281/zenodo.5563009

Oskinova LM, Todt H, Ignace R, et al (2011) Early magnetic B-type stars: X-ray emission and wind properties. $MNRAS$416(2):1456–1474. https://doi.org/10.1111/j.1365-2966.2011.19143.x, https://arxiv.org/abs/arXiv:1106.0508 [astro-ph.SR]

Owocki SP (2018) Hot-Star Winds: CIRs, DACs & BRITE Spots. In: Wade GA, Baade D, Guzik JA, et al (eds) 3rd BRITE Science Conference, pp 48–56

Owocki SP, Castor JI, Rybicki GB (1988) Time-dependent Models of Radiatively Driven Stellar Winds. I. Nonlinear Evolution of Instabilities for a Pure Absorption Model. ApJ335:914. https://doi.org/10.1086/166977

Owocki SP, ud-Doula A, Sundqvist JO, et al (2016) An 'analytic dynamical magneto-sphere' formalism for X-ray and optical emission from slowly rotating magnetic massive stars. $MNRAS$462(4):3830–3844. https://doi.org/10.1093/mnras/stw1894, https://arxiv.org/abs/arXiv:1607.08568 [astro-ph.SR]

Owocki SP, Shultz ME, ud-Doula A, et al (2020) How the breakout-limited mass in B-star centrifugal magnetospheres controls their circumstellar H α emission. $MNRAS$499(4):5366–5378. https://doi.org/10.1093/mnras/staa2325, https://arxiv.org/abs/arXiv:2009.12359 [astro-ph.SR]

Petit V, Massa DL, Marcolino WLF, et al (2011) Discovery of the first τ Sco analogues: HD 66665 and HD 63425. $MNRAS$412:L45–L49. https://doi.org/10.1111/j.1745-3933.2010.01002.x, https://arxiv.org/abs/arXiv:1012.4445 [astro-ph.SR]

Petit V, Owocki SP, Wade GA, et al (2013) **P13:** A magnetic confinement versus rotation classification of massive-star magnetospheres. $MNRAS$429:398–422. https://doi.org/10.1093/mnras/sts344, https://arxiv.org/abs/arXiv:1211.0282 [astro-ph.SR]

Petit V, Cohen DH, Wade GA, et al (2015) X-ray emission from the giant magneto-sphere of the magnetic O-type star NGC 1624-2. $MNRAS$453(3):3288–3299. https://doi.org/10.1093/mnras/stv1741, https://arxiv.org/abs/arXiv:1507.08621 [astro-ph.SR]

Petit V, Keszthelyi Z, MacInnis R, et al (2017) Magnetic massive stars as progenitors of 'heavy' stellar-mass black holes. $MNRAS$466(1):1052–1060. https://doi.org/10.1093/mnras/stw3126, https://arxiv.org/abs/arXiv:1611.08964 [astro-ph.SR]

Ramiaramanantsoa T, Moffat AFJ, Chené AN, et al (2014) MOST detects coro-tating bright spots on the mid-O-type giant ξ Persei. $MNRAS$441:910–917. https://doi.org/10.1093/mnras/stu619, https://arxiv.org/abs/arXiv:1403.7843 [astro-ph.SR]

Ramiaramanantsoa T, Moffat AFJ, Harmon R, et al (2018) BRITE-Constellation high-precision time-dependent photometry of the early O-type supergiant ζ Puppis unveils the photospheric drivers of its small- and large-scale wind structures. $MNRAS$473:5532–5569. https://doi.org/10.1093/mnras/stx2671, https://arxiv.org/abs/arXiv:1710.08414 [astro-ph.SR]

Rauw G, Hervé A, Nazé Y, et al (2015) Simultaneous X-ray and optical spectroscopy of the Oef supergiant λ Cephei. A&A580:A59. https://doi.org/10.1051/0004-6361/201526057, https://arxiv.org/abs/arXiv:1505.07714 [astro-ph.SR]

Renedo I, Althaus LG, Miller Bertolami MM, et al (2010) New Cooling Sequences for Old White Dwarfs. ApJ717(1):183–195. https://doi.org/10.1088/0004-637X/717/1/183, https://arxiv.org/abs/arXiv:1005.2170 [astro-ph.SR]

Schneider FRN, Ohlmann ST, Podsiadlowski P, et al (2019) Stellar mergers as the origin of magnetic massive stars. Nature574(7777):211–214. https://doi.org/10.1038/s41586-019-1621-5, https://arxiv.org/abs/arXiv:1910.14058

[astro-ph.SR]

Schnerr RS, Henrichs HF, Neiner C, et al (2008) Magnetic field measurements and wind-line variability of OB-type stars. A&A483(3):857–867. https://doi.org/10.1051/0004-6361:20077740, https://arxiv.org/abs/arXiv:1008.4260 [astro-ph.SR]

Schöller M, Hubrig S, Fossati L, et al (2017) B fields in OB stars (BOB): Concluding the FORS 2 observing campaign. A&A599:A66. https://doi.org/10.1051/0004-6361/201628905, https://arxiv.org/abs/arXiv:1611.04502 [astro-ph.SR]

Scowen PA, Gayley K, Neiner C, et al (2021) The Polstar High Resolution Spectropolarimetry MIDEX Mission. In: Society of Photo-Optical Instrumentation Engineers (SPIE) Conference Series, p 1181908, https://doi.org/10.1117/12.2594267, 2108.10729

Shore SN, Brown DN (1990) Magnetically Controlled Circumstellar Matter in the Helium-strong Stars. ApJ365:665. https://doi.org/10.1086/169520

Shultz M, Wade GA (2017) Confirming the oblique rotator model for the extremely slowly rotating O8f?p star HD 108. MNRAS468(4):3985–3992. https://doi.org/10.1093/mnras/stx759, https://arxiv.org/abs/arXiv:1703.08996 [astro-ph.SR]

Shultz M, Wade GA, Rivinius T, et al (2017) The pulsating magnetosphere of the extremely slowly rotating magnetic β Cep star ξ^1 CMa. MNRAS471:2286–2310. https://doi.org/10.1093/mnras/stx1632, https://arxiv.org/abs/arXiv:1706.08820 [astro-ph.SR]

Shultz ME, Wade GA, Rivinius T, et al (2018) The magnetic early B-type stars I: magnetometry and rotation. MNRAS475:5144–5178. https://doi.org/10.1093/mnras/sty103, https://arxiv.org/abs/arXiv:1801.02924 [astro-ph.SR]

Shultz ME, Wade GA, Rivinius T, et al (2019) The magnetic early B-type stars - III. A main-sequence magnetic, rotational, and magnetospheric biography. MNRAS490(1):274–295. https://doi.org/10.1093/mnras/stz2551, https://arxiv.org/abs/arXiv:1909.02530 [astro-ph.SR]

Shultz ME, Owocki S, Rivinius T, et al (2020) The magnetic early B-type stars - IV. Breakout or leakage? H α emission as a diagnostic of plasma transport in centrifugal magnetospheres. MNRAS499(4):5379–5395. https://doi.org/10.1093/mnras/staa3102, https://arxiv.org/abs/arXiv:2009.12336 [astro-ph.SR]

Shulyak D, Reiners A, Engeln A, et al (2017) Strong dipole magnetic fields in fast rotating fully convective stars. Nature Astronomy 1:0184. https://doi.org/10.1038/s41550-017-0184, https://arxiv.org/abs/arXiv:1801.08571 [astro-ph.SR]

Sikora J, Wade GA, Power J, et al (2019) A volume-limited survey of mCP stars within 100 pc II: rotational and magnetic properties. MNRAS483(3):3127–3145. https://doi.org/10.1093/mnras/sty2895, https://arxiv.org/abs/arXiv:1811.05635 [astro-ph.SR]

Slane P, Bykov A, Ellison DC, et al (2016) Supernova Remnants Interacting with Molecular Clouds: X-Ray and Gamma-Ray Signatures. In: Balogh A, Bykov A, Eastwood J, et al (eds) Multi-scale Structure Formation and Dynamics in Cosmic Plasmas, vol 51. p 187, https://doi.org/10.1007/978-1-4939-3547-5_6

Slettebak A (1994) Ultraviolet Spectral Classification and Stellar Winds in a Sample of Be and Standard Stars. ApJS94:163. https://doi.org/10.1086/192077

Smith MA, Fullerton AW (2005) A Revised Geometry for the Magnetic Wind of θ^1 Orionis C. PASP117(827):13–21. https://doi.org/10.1086/427538, https://arxiv.org/abs/arXiv:astro-ph/0412150

[astro-ph]

Smith MA, Groote D (2001) Wind circulation in selected rotating magnetic early-B stars. A&A372:208–226. https://doi.org/10.1051/0004-6361:20010472, https://arxiv.org/abs/arXiv:astro-ph/0104059 [astro-ph]

Sudnik NP, Henrichs HF (2016) Multiple short-lived stellar prominences on O stars: The O6.5I(n)fp star λ Cephei. A&A594:A56. https://doi.org/10.1051/0004-6361/201628529, https://arxiv.org/abs/arXiv:1606.00404 [astro-ph.SR]

Sundqvist JO, ud-Doula A, Owocki SP, et al (2012) A dynamical magnetosphere model for periodic Hα emission from the slowly rotating magnetic O star HD 191612. $MNRAS$423(1):L21–L25. https://doi.org/10.1111/j.1745-3933.2012.01248.x, https://arxiv.org/abs/arXiv:1203.1050 [astro-ph.SR]

Townsend RHD, Owocki SP, Groote D (2005) The Rigidly Rotating Magnetosphere of σ Orionis E. $ApJL$630(1):L81–L84. https://doi.org/10.1086/462413, https://arxiv.org/abs/arXiv:astro-ph/0503668 [astro-ph]

Townsend RHD, Oksala ME, Cohen DH, et al (2010) Discovery of Rotational Braking in the Magnetic Helium-strong Star Sigma Orionis E. $ApJL$714(2):L318–L322. https://doi.org/10.1088/2041-8205/714/2/L318, https://arxiv.org/abs/arXiv:1004.2038 [astro-ph.SR]

ud-Doula A (2020) 3D MHD Simulations of Obliquely Rotating Massive Stars. In: Wade G, Alecian E, Bohlender D, et al (eds) Stellar Magnetism: A Workshop in Honour of the Career and Contributions of John D. Landstreet, pp 140–147

ud-Doula A, Nazé Y (2016) Magnetically confined wind shocks in X-rays - A review. Advances in Space Research 58(5):680–693. https://doi.org/10.1016/j.asr.2015.09.025, https://arxiv.org/abs/arXiv:1509.06482

[astro-ph.SR]

ud-Doula A, Owocki SP (2002) Dynamical Simulations of Magnetically Channeled Line-driven Stellar Winds. I. Isothermal, Nonrotating, Radially Driven Flow. ApJ576(1):413–428. https://doi.org/10.1086/341543, https://arxiv.org/abs/arXiv:astro-ph/0201195 [astro-ph]

ud-Doula A, Owocki SP, Townsend RHD (2008) Dynamical simulations of magnetically channelled line-driven stellar winds - II. The effects of field-aligned rotation. $MNRAS$385(1):97–108. https://doi.org/10.1111/j.1365-2966.2008.12840.x, https://arxiv.org/abs/arXiv:0712.2780 [astro-ph]

ud-Doula A, Owocki SP, Townsend RHD (2009) Dynamical simulations of magnetically channelled line-driven stellar winds - III. Angular momentum loss and rotational spin-down. $MNRAS$392(3):1022–1033. https://doi.org/10.1111/j.1365-2966.2008.14134.x, https://arxiv.org/abs/arXiv:0810.4247 [astro-ph]

ud-Doula A, Sundqvist JO, Owocki SP, et al (2013) First 3DMHD simulation of a massive-star magnetosphere with application to Hα emission from θ^1 Ori C. $MNRAS$428(3):2723–2730. https://doi.org/10.1093/mnras/sts246, https://arxiv.org/abs/arXiv:1210.5298 [astro-ph.SR]

ud-Doula A, Owocki S, Townsend R, et al (2014a) X-rays from magnetically confined wind shocks: effect of cooling-regulated shock retreat. $MNRAS$441:3600–3614. https://doi.org/10.1093/mnras/stu769, https://arxiv.org/abs/arXiv:1404.5336 [astro-ph.SR]

ud-Doula A, Owocki S, Townsend R, et al (2014b) X-rays from magnetically confined wind shocks: effect of cooling-regulated shock retreat. $MNRAS$441(4):3600–3614. https://doi.org/10.1093/mnras/stu769, https://arxiv.org/abs/arXiv:1404.5336 [astro-ph.SR]

Villebrun F, Alecian E, Hussain G, et al (2019) Magnetic fields of intermediate-mass T Tauri stars. I. Magnetic detections and fundamental stellar parameters. A&A622:A72. https://doi.org/10.1051/0004-6361/201833545, https://arxiv.org/abs/arXiv:1810.12803 [astro-ph.SR]

Vink JS, Drew JE, Harries TJ, et al (2002) Probing the circumstellar structure of Herbig Ae/Be stars. $MNRAS$337(1):356–368. https://doi.org/10.1046/j.1365-8711.2002.05920.x, https://arxiv.org/abs/arXiv:astro-ph/0208137 [astro-ph]

Vink JS, Drew JE, Harries TJ, et al (2005a) Probing the circumstellar structures of T Tauri stars and their relationship to those of Herbig stars. $MNRAS$359(3):1049–1064. https://doi.org/10.1111/j.1365-2966.2005.08969.x, https://arxiv.org/abs/arXiv:astro-ph/0502535 [astro-ph]

Vink JS, Harries TJ, Drew JE (2005b) Polarimetric line profiles for scattering off rotating disks. A&A430:213–222. https://doi.org/10.1051/0004-6361:20041463, https://arxiv.org/abs/arXiv:astro-ph/0409512 [astro-ph]

von Zeipel H (1924) The radiative equilibrium of a rotating system of gaseous masses. $MNRAS$84:665–683. https://doi.org/10.1093/mnras/84.9.665

Wade GA, Maíz Apellániz J, Martins F, et al (2012) NGC 1624-2: a slowly rotating, X-ray luminous Of?cp star with an extraordinarily strong magnetic field. $MNRAS$425(2):1278–1293. https://doi.org/10.1111/j.1365-2966.2012.21523.x, https://arxiv.org/abs/arXiv:1206.2834 [astro-ph.SR]

Wood K, Brown JC, Fox GK (1993) Polarimetric line profiles from optically thin Thomson scattering circumstellar envelopes. A&A271:492

Yakunin I, Wade G, Bohlender D, et al (2015) The surface magnetic field and chemical abundance distributions of the B2V helium-strong star HD 184927. $MNRAS$447(2):1418–1438. https://doi.org/10.1093/mnras/stu2401, https://arxiv.org/abs/arXiv:1411.5789 [astro-ph.SR]

Statements & Declarations

Competing Interests

The authors have no relevant financial or non-financial interests to disclose.

Author Contributions

All authors contributed to the study conception and design. The first draft of the manuscript was written by Asif ud-Doula and all authors commented on previous versions of the manuscript. All authors read and approved the final manuscript.

Data availability

Data sharing not applicable to this article as no datasets were generated or analysed during the current study.

Affiliations

[1]Penn State Scranton, 120 Ridge View Drive, Dunmore, PA 18512, US

[2]Lockheed Martin Solar and Astrophysics Laboratory, 3251 Hanover St, Palo Alto, CA 94304, USA

[3]Department of Physics and Astronomy, Howard University, Washington, DC 20059, USA

[4]Center for Research and Exploration in Space Science and Technology, and X-ray Astrophysics Laboratory, NASA/GSFC, Greenbelt, MD 20771, USA

[5]Department of Physics & Astronomy, East Tennessee State University, Johnson City, TN 37614, USA

[6]Tartu Observatory, University of Tartu, Observatooriumi 1, Tõravere, 61602, Estonia

[7]Department of Physics & Astronomy, University of Iowa, 203 Van Allen Hall, Iowa City, IA, 52242, USA

[8]GAPHE, Université de Liège, Allée du 6 Août 19c (B5C), B-4000 Sart Tilman, Liège, Belgium

[9]LESIA, Paris Observatory, PSL University, CNRS, Sorbonne University, Université de Paris, 5 place Jules Janssen, 92195 Meudon, France

[10]Department of Physics and Astronomy, University of Delaware, 217 Sharp Lab, Newark, Delaware, 19716, USA

[11]Department of Physics and Astronomy, Gower Street, London WC1E 6BT, UK

[12]Nicolaus Copernicus Astronomical Centre of the Polish Academy of Sciences, Bartycka 18, 00-716 Warsaw, Poland

[13]Armagh Observatory and Planetarium, College Hill, BT61 9DG Armagh, Northern Ireland

[14]Department of Physics and Space Science, Royal Military College of Canada, PO Box 17000, Station Forces, Kingston, ON, K7K 7B4